

KINETIC MODELLING OF ETHANOL
PRODUCTION FROM OIL PALM TRUNK SAP
DURING FERMENTATION

SHARMIN SULTANA

UMP

MASTER OF SCIENCE

UNIVERSITI MALAYSIA PAHANG

UNIVERSITI MALAYSIA PAHANG

DECLARATION OF THESIS AND COPYRIGHT

Author's Full Name : SHARMIN SULTANA

Date of Birth : 25/12/1986

Title : KINETIC MODELLING OF ETHANOL PRODUCTION
FROM OIL PALM TRUNK SAP DURING
FERMENTATION

Academic Session : SEM 2/2018/2019

I declare that this thesis is classified as:

- CONFIDENTIAL (Contains confidential information under the Official Secret Act 1997)*
- RESTRICTED (Contains restricted information as specified by the organization where research was done)*
- OPEN ACCESS I agree that my thesis to be published as online open access (Full Text)

I acknowledge that Universiti Malaysia Pahang reserves the following rights:

1. The Thesis is the Property of Universiti Malaysia Pahang
2. The Library of Universiti Malaysia Pahang has the right to make copies of the thesis for the purpose of research only.
3. The Library has the right to make copies of the thesis for academic exchange.

Certified by:



(Student's Signature)

BN0531273

New IC/Passport Number
Date:20/05/2019

(Supervisor's Signature)

Dr Norazaliza Binti Mohd Jamil

Name of Supervisor
Date:

NOTE : * If the thesis is CONFIDENTIAL or RESTRICTED, please attach a thesis declaration letter.

SUPERVISOR'S DECLARATION

We hereby declare that we have checked this thesis and in our opinion, this thesis is adequate in terms of scope and quality for the award of the degree of Master of Science.

(Supervisor's Signature)

Full Name : DR NORAZALIZA BINTI MOHD JAMIL

Position : SENIOR LECTURER

Date :

(Co-supervisor's Signature)

Full Name : DR. ESSAM ABDELLATIF MAKKY SALEH

Position : ASSOCIATE PROFESSOR

Date :

STUDENT'S DECLARATION

I hereby declare that the work in this thesis is based on my original work except for quotations and citations which have been duly acknowledged. I also declare that it has not been previously or concurrently submitted for any other degree at Universiti Malaysia Pahang or any other institutions.



(Student's Signature)

Full Name : SHARMIN SULTANA

ID Number : MPE15002

Date :



UMP

KINETIC MODELLING OF ETHANOL PRODUCTION FROM OIL PALM TRUNK
SAP DURING FERMENTATION



SHARMIN SULTANA

Thesis submitted in fulfilment of the requirements
for the award of the degree of
Master of Science

UMP
Faculty of Industrial Sciences & Technology
UNIVERSITI MALAYSIA PAHANG

JULY 2019

ACKNOWLEDGEMENT

The study presented in this thesis has been carried out at the Faculty of Industrial Science and Technology, Universiti Malaysia Pahang, Malaysia. The journey of my research would not be possible without help and support of a number of persons.

First and foremost, my heart-full gratitude to Almighty Allah SWT, who allow me physical and mental soundness and fitness to do the research work. After that, I wish to my humble gratefulness and sincere thanks to honourable supervisor, Dr. Norazaliza Binti Mohd Jamil for her valuable support and guidance throughout the study. Indeed, it was utmost opportunity for me to get her as my main supervisor. She has always been able to keep on amazing me with her thoughtful ideas and insights. I would also like to give special thanks to my co-supervisors, Dr. Essam Abdellatif Makky Saleh for his support.

Apart from that, I am highly grateful to the Universiti Malaysia Pahang (UMP), Malaysia, for funding this work under the research grant RDU150399. I would like to acknowledge the tremendous support of Dr Che Ku M Faizal, Faculty of Engineering Technology, University Malaysia Pahang for sharing the experimental data of OPT sap fermentation.

Special thanks must be given to Sadekur Rahman, Mr. Ahasanul Karim, Dr Amirul Islam and Jahan Ali for their kind help and suggestion throughout the research work.

Lastly, I also want to thank to my parents and family for their continuous supports, encouragements and inspirations. It would be really tough to finish my study without their supports and devotions.



UMP

ABSTRAK

Penyimpanan bahan api fosil di seluruh dunia yang terhad dan impaknya yang buruk terhadap alam sekitar membawa kepada penyelidikan terkini ke arah penggunaan biomas dalam penghasilan biofuel. Malaysia kaya dengan sumber biomas. Batang kelapa sawit (OPT) adalah sumber biomas untuk menghasilkan bioethanol. Fermentasi adalah proses terpenting dalam penukaran biomas kepada etanol. Model kinetik yang sesuai mampu meningkatkan kecekapan dan proses pengoptimuman penapaian etanol menggunakan sap OPT. Kaedah teoritikal lebih efisien dan memerlukan kos pelaburan yang rendah, tetapi kaedah ini sukar untuk disahkan. Beberapa model kinetik telah dicadangkan tetapi tiada model yang mengambil kira faktor-faktor penting seperti batasan substrat, perencat substrat, penghambatan produk, dan kematian sel secara serentak pada suhu berbeza untuk menghasilkan etanol dari penapaian sap OPT. Kami memanjangkan dan memperbaiki model matematik terkini untuk meneroka kesan suhu, kepekatan sel terawal dan kadar kematian sel pada proses penapaian. Beberapa parameter kinetik digunakan untuk menggambarkan fenomena ini. Satu set persamaan pembezaan biasa digunakan untuk memodelkan profil gula, sel dan etanol untuk penapaian sap OPT dan persamaan telah diselesaikan oleh kaedah Runge-Kutta untuk ke-4. Terdapat dua set hasil simulasi yang dibentangkan dalam kajian ini untuk Model I dan II. Model I adalah model mudah yang memanjangkan model Oliviera, di mana kami mengkaji kesan kadar kematian sel. Model II lebih komprehensif dan lebih baik daripada Model I, kerana ia mempunyai hubungan Leudeking-Piret, model Phisalaphong dan juga Model I. Seseengah ciri-ciri penting dikenalpasti kedua-dua model. Apabila suhu meningkat, kadar pertumbuhan sel khusus maksimum menurun bagi kedua-dua model. Dari hasilnya, Suhu yang sesuai untuk pengeluaran etanol dari penapaian sap OPT ialah 30°C. Kadar penggunaan gula dan pengeluaran etanol sepanjang proses penapaian bergantung pada kepekatan sel awal. Dengan kepekatan sel awal yang rendah, kadar penukaran meningkat secara beransur-ansur tetapi untuk kepekatan sel awal yang tinggi, penukaran gula ke etanol meningkat dengan ketara dan berkurangan selepas tempoh yang singkat disebabkan oleh akses etanol, yang mungkin menghalang pertumbuhan sel. Pertimbangan gabungan batasan dan perencatan substrat, penghambatan produk dan kadar kematian sel meningkatkan ketepatan model I dengan cara rRMSE. Pemerhatian serupa ditemui untuk model II apabila faktor-faktor yang dipertimbangkan adalah had dan penyekatan substrat, pertumbuhan dan pembentukan produk yang berkaitan dengan pertumbuhan, penghambatan produk dan kematian sel. Pendekatan ini membolehkan kita memperoleh keupayaan ramalan yang lebih baik dengan itu meningkatkan pemahaman kita terhadap model matematik penapaian sap OPT.

ABSTRACT

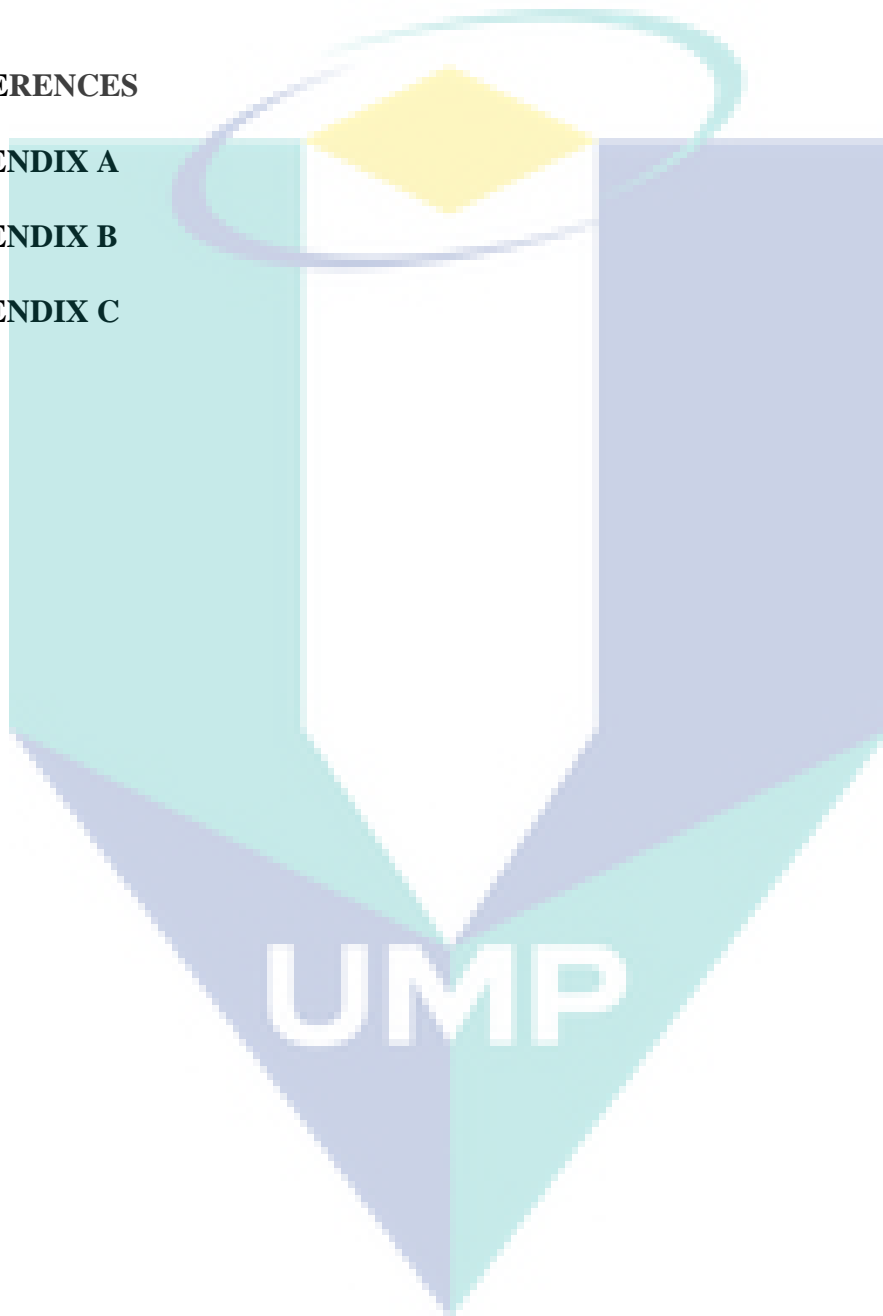
The worldwide limited storage of fossil fuel and its bad impact on environment lead to the recent research towards biomass for biofuel. Malaysia is rich with plenty of biomass resources. Oil palm trunk (OPT) is a promising biomass source for bioethanol production. Fermentation is an essential process of biomass to ethanol conversion. An appropriate kinetic model will be a powerful tool to increase the efficiency and process optimization for ethanol fermentation using the OPT sap. The theoretical methods are more efficient and require low investment, but it is challenging to validate. A number of kinetic models have been proposed but none of these models observed the effect of most essential factors such as substrate limitation, substrate inhibition, product inhibition, and cell death simultaneously on temperature to produce ethanol from the OPT sap fermentation. We extended and improved the current mathematical model to explore the effect of temperature, initial cell concentration and cell death rate on the fermentation process. Several kinetic parameters were used to describe this phenomenon. A set of ordinary differential equations were used to modelled the profiles of sugar, cell and ethanol for the fermentation of OPT sap and the equations were solved by the 4th order Runge-Kutta method. There are two sets of simulation results presented in this study for Model I and II. Model I is a simple model which extends Oliviera's model, where we studied the effect of cell death rate. Model II is more comprehensive and better than Model I, because it consists Leudeking-Piret relationship, Phisalaphong model and also Model I. Some significant characteristics are apprehended both of the models. As the temperature increased, the maximum specific cell growth rate decreased for both of the models. From the results, the suitable temperature for ethanol production from the OPT sap fermentation is 30°C. The rate of sugar utilisation and ethanol production throughout fermentation process depend on the initial cell concentration. With the low initial cell concentration, the conversion rate was increased gradually but for the high initial cell concentration, sugar conversion to ethanol was augmented sharply and depleted after the short duration due to access of the ethanol, which might inhibit the cell growth. The combined consideration of the substrate limitation and inhibition, growth and non-growth associated product formation, product inhibition and cell death rate increased the accuracy of the Model II by means of rRMSE. This approach has enabled us to obtained a better predictive capabilities hence increasing our understanding of the mathematical model of the OPT sap fermentation.

TABLE OF CONTENTS

DECLARATION	
TITLE PAGE	
SUPERVISOR'S DECLARATION	
STUDENT'S DECLARATION	
ACKNOWLEDGEMENT	ii
ABSTRAK	iii
ABSTRACT	iv
TABLE OF CONTENTS	v
LIST OF TABLES	viii
LIST OF FIGURES	ix
LIST OF SYMBOLS	x
CHAPTER 1 INTRODUCTION	1
1.1 Research Background	1
1.2 Problem Statement	2
1.3 Research Objectives	3
1.4 Research Scope	4
1.5 Research Significance	5
1.6 Thesis outline	5
CHAPTER 2 LITERATURE REVIEW	6
2.1 Introduction	6
2.2 Fermentation Process	7
2.3 Kinetic Modeling of Ethanol Fermentation	8

2.4 Kinetic Model by Phisalaphong	13
2.5 Kinetic Model by Oliviera	15
2.6 Kinetic Model by Leudeking-Piret relationship	16
2.7 Summary	17
CHAPTER 3 MATHEMATICAL MODELLING AND NUMERICAL SOLUTION	18
3.1 Introduction	18
3.2 Model I	18
3.3 Model II	20
3.4 Data description	23
3.5 Numerical solution	24
3.6 Runge-Kutta method	25
3.6.1 Model I.	26
3.6.2 Model II	28
3.7 Parameter estimation	29
3.7.1 Nelder-Mead simplex algorithm	30
3.8 Flow chart of numerical solution	31
3.9 Summary	32
CHAPTER 4 RESULTS AND DISCUSSION	33
4.1 Introduction	33
4.2 Model I: Simulated result	33
4.3 Model II: Simulated result	38
4.4 Effect of initial cell concentration	43
4.5 Summary	45

CHAPTER 5 CONCLUSION	47
5.1 Introduction	47
5.2 Conclusion	47
5.3 Recommendations for Future Research	48
REFERENCES	50
APPENDIX A	55
APPENDIX B	69
APPENDIX C	83



LIST OF TABLES

Table 3.1	Summary of mathematical models	21
Table 4.1	Values of the kinetic parameters at different temperature estimated by nonlinear regression	34
Table 4.2	Comparison of relative root mean squared error (rRMSE) for accuracy of the proposed model (Model I) with Oliveira's model	37
Table 4.3	Values of the kinetic parameters at different temperature estimated by nonlinear regression	39
Table 4.4	Accuracy of the proposed model considering (rRMSE)	42



UMP

LIST OF FIGURES

Figure 2.1	Steps of OPT processing to bioethanol	7
Figure 3.1	OPT sap preparation and fermentation	23
Figure 3.2	Flow chart of numerical solution	31
Figure 4.1	Experimental data and model predictions of batch fermentation at 25°C temperature	35
Figure 4.2	Experimental data and model predictions of batch cultivations at 30°C temperature	36
Figure 4.3	Experimental data and model predictions of batch cultivations at 35°C temperature	36
Figure 4.4	Arrhenius plots illustrating the effect of temperature on (a) the maximum specific growth rate (μ_{max})	40
Figure 4.5	Experimental data and model predictions of batch fermentation at 25°C temperature	41
Figure 4.6	Experimental data and model predictions of batch fermentation at 30°C temperature	41
Figure 4.7	Experimental data and model predictions of batch fermentation at 35°C temperature	42
Figure 4.8	Sugar to ethanol conversion at different initial cell concentration: 1, 2 and 3g/L.	43
Figure 4.9	Sugar to ethanol conversion for 25°C at different initial cell concentration: 10, 15 and 20g/L.	44
Figure 4.10	Sugar to ethanol conversion for 30°C at different initial cell	45
Figure 4.11	Sugar to ethanol conversion for 35°C at different initial cell concentration: 10, 15 and 20g/L.	45

LIST OF SYMBOLS

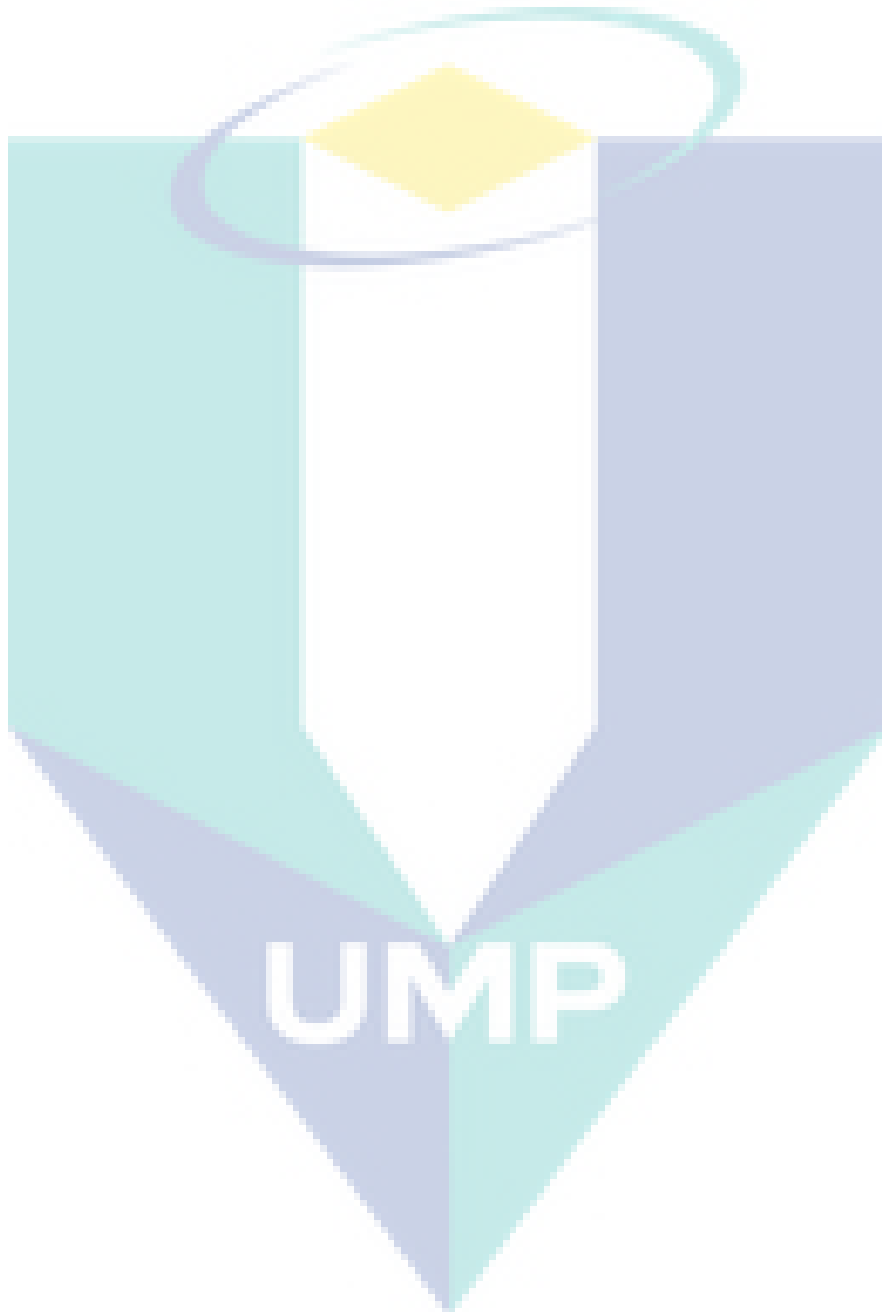
a	growth associated specific productivity coefficient
b	Non-growth associated specific productivity coefficient
c	Coefficient of cell maintenance
$f(x_i)$	Calculated data
K_{CM}	Maintenance constant
K_d	Cell death rate
K_i	Substrate inhibition coefficient/ Inhibition parameter for sugar
K_S	Saturation constant of substrate/ Substrate inhibition constant
$K_{in,S}$	Substrate inhibition constant
$K_{li,S}$	Substrate limitation constant
K_{li,O_2}	Dissolved oxygen limitation constant
K_P	Product inhibition constant
K_{SP}	Saturation constant for ethanol production
K_{SS}	Substrate inhibition term for cell growth
K_{SSP}	Substrate inhibition term for ethanol production
n	Ethanol toxic power
O_2	Dissolved oxygen concentration
P	Ethanol production
P_m	Ethanol inhibition term for cell growth
P'_M	Ethanol inhibition term for ethanol production
P^*	Critical concentration of product
r	Reaction rate
$Y'_{x/s}, Y_{x/s}$	Yield coefficient for the cell on substrate
$Y'_{p/s}, Y_{p/s}$	Yield coefficient for the ethanol on substrate
y_i	Experimental data
α	Model parameter
μ	Specific growth rate

$\hat{\mu}$

Maximum specific growth rate

ν

Specific production rate



CHAPTER 1

INTRODUCTION

1.1 Research Background

The economic growth, changing consumption and production patterns of goods result in energy crises and environmental pollution, which have become vital problems to the human society. The rapid industrialization has increased the demand for fuel. However, the energy supply from fossil fuels worldwide is limited and will eventually be depleted. In the last century the energy consumption has increased to 17-fold with the present rate of energy consumption, it is predictable that the world's oil reservoir will be diminished by 2050 (Alauddin et al. 2010). The combustion of fossil fuels produces large amount of carbon dioxide (CO₂) causing greenhouse effect and global warming. Meanwhile, the cost of fossil fuel is generally increasing. These issues remind us the need to find alternative fuel resources which are renewable and counted as eco-friendly.

The lignocellulosic biomass feedstock include palm trees, agricultural residues, energy crops (e.g., switch grass, miscanthus, energy cane, sorghum, polar, and willow) forest resources (e.g., forest thinning, wood chips, wood wastes, small diameter trees) and urban wood waste (Zhang 2011). The conversion of biomass to ethanol involves a large number of physical and chemical transformations. This biomass can be converted into energy products in biochemical process such as fermentation, and thermochemical processes such as combustion, pyrolysis and gasification (Wang et al. 2015) and the resulting fuels are alcohols, biodiesels, syngas and briquette. The chemical properties of biomass material are complex and the reaction kinetics for the degradation of biomass is not well understood (Jamil and Wang 2016). For this reason, in order to understand, to operate, to optimize and to control ethanol fermentation process, a more complete knowledge of dynamic behavior is required (Oliveira et al. 2016).

In Malaysia, oil palm tree has become the main source of biomass to produce renewable energy. The palm oil industry is very important in Malaysia as the country has maintained its position as the world's leading palm oil producing country. The main products of palm oil processing are foods, oleo chemicals and renewable energy source. Ongoing research and development of palm biomass by governmental institutions and universities improves process efficiencies (You and Baharin 2006).

Ethanol is an interesting fuel which supports a sustainable economy by reducing the use of petroleum, carbon dioxide (CO₂) accumulation particulate matter and nitrous/nitric oxide (NO_x) emission from combustion (Srimachai et al. 2015). The production of ethanol from lignocellulosic biomass consists of three fundamental processes; pretreatment, hydrolysis, and fermentation (Limayem and Ricke 2012). Pretreatment modifies the structure of biomass to make the cellulose more exposed to enzymes for sugar conversion (Himmel et al. 2007). Hydrolysis breaks cellulose chains into sugar such as cellobiose and glucose, whereas fermentation converts sugar into ethanol.

The fermentation step is an essential part of biomass to ethanol conversion process. An appropriate kinetic model of ethanol fermentation would be a powerful instrument for increasing fermentation efficiency and process optimization (Liu and Li 2014). Fermentation kinetic model is an important tool to describe the yeast behavior, metabolism and bioethanol regulation (Phisalaphong et al. 2006).

To date, it was found that most of the current researches done to produce bioethanol from OPT sap are only employing *Saccharomyces cerevisiae* as the fermentative microbe (Halim 2016). The necessity to select suitable bacteria or yeast is important to enhance the production of bioethanol to make it economically feasible. Therefore, in this study we will focus most specifically on the mathematical model that would thoroughly describe the kinetics of cell (*Saccharomyces cerevisiae*) and sugar activities in the OPT sap from the beginning up to the stationary phase in order to maximize the production of ethanol during fermentation process.

1.2 Problem Statement

There are two research methods on biomass conversion, which are experimental and theoretical. Experimental studies can give the results directly and accurately to

determine the production process, but the investment is large. On the other hand, the theoretical methods in terms of mathematical are simpler, more efficient and require smaller investment, but it is challenging to validate, as there is a big gap compared to the actual results. Therefore, more accurate mathematical model becomes particularly important. It cannot be expected that any kinetic model will be directly applicable to a real process situation. Therefore, mathematical modelling should start with the simplest type, but it must be repeated, modified and extended until it eventually leads to an acceptable process kinetic model (Birol et al. 1998).

A number of mathematical models for fermentation process have been proposed, for example by Esfahanian et al. (2016); Hinshelwood (1946); Ghose and Tyagi (1979); Jin et al. (2012); Liu and Li (2014); (Monod 1949b); and Oliveira et al. (2016); to predict the effect of operating parameters on cell growth, substrate utilization rate and ethanol production rate. Some of them focused only the single factor, other researchers focused more than one factors. But none of them considered OPT sap as a substrate. Although there are many studies on kinetic has existed for microbial activities in bioethanol research area, reasonable kinetic parameter values were not always accurately estimated (Halim 2016). The essential factors such as substrate limitation, substrate inhibition, product inhibition, and cell death are known to affect ethanol fermentation process, but none of the previous models accounts those kinetic factors simultaneously. Optimization of important parameters can reduce cost and provides more accurate results for the ethanol production process. That is why, to show the effect of culture parameters such as temperature and initial cell concentration are being considered. Therefore, an appropriate ethanol fermentation model should account those kinetic factors. However, to the best our knowledge, there are no literature reports accounting those factors all together for the kinetic performance by *Saccharomyces cerevisiae* on the oil palm trunk (OPT) sap fermentation.

1.3 Research Objectives

This research is concerned with the study of kinetic parameters of ethanol production during batch fermentation. Thus, the objectives of this research are:

- i) To modify a mathematical model that is capable of predicting the changes of ethanol, cell and substrate concentrations considering the substrate

limitation, substrate inhibition, product inhibition, and cell death during the batch fermentation process using OPT sap.

- ii) To solve the mathematical model by using the 4th order Runge-Kutta method.
- iii) To investigate the effect of temperature, cell death and initial cell concentration on fermentation process.

1.4 Research Scope

Fermentation kinetic model is an important tool to describe the yeast behavior, metabolism and bioethanol regulation. The growth of microbial cell can be described by the structured and unstructured model during fermentation. The unstructured models which describe microbial kinetics include the most fundamental observations relating microbial growth processes like biomass concentration, substrate consumption and synthesize metabolic products (Vázquez and Murado 2008). The unstructured kinetic models describe the principal kinetics involved in the ethanol fermentation (Fan et al. 2015). The unstructured models simply view the cell as a unit in solution which interacts with the environment. The structured models consider individual reaction or group of reactions that occur within the cell.

Compared to the unstructured kinetic models, structured models are usually complicated to estimate the kinetic parameters, mainly because of nonlinearities, the large number of parameters, and interactions among complex microbial systems at the molecular level such as DNA, RNA, protein etc (Rivera et al. 2008). For this reason, relatively simple unstructured kinetic models such as the Monod model and Luedeking–Piret (LP) model have frequently been used for practical application (Wang and Liu 2014). Hence an unstructured comprehensive kinetic model was proposed in this study that is modified from the Monod kinetics which responds to the changes in the environmental conditions of fermentation.

To our knowledge, no investigations have been carried out on the unstructured model for ethanol fermentation from OPT sap. In this research, the kinetic model is applied to the experimental data from batch fermentations of ethanol from the OPT sap using *Saccharomyces cerevisiae*.

1.5 Research Significance

The proposed mathematical model will help to predict the production yield of ethanol. This study will contribute a better understanding of the environmental changes in fermentation process, which can serve as guidance to further optimize the ethanol fermentation process. Besides that, when any fermentation process may scale-up from small scale to large scale, the model can explain the kinetic behaviour of cell. This fermentation kinetic model is using the OPT sap as nutrient which will be beneficial for some organizations such as the Forest Research Institute Malaysia (FRIM), Palm Oil Research Institute of Malaysia (PORIM), Malaysian Agriculture Research and Development Institute (MARDI) and Ministry of Agriculture (MA). They can use our model using some process parameter, such as temperature, initial values of cell and significant nutrient to generate good amount of bioethanol by minimizing the production cost.

1.6 Thesis outline

The thesis paper has been composed by five chapters. Such as introduction, Literature Review, Mathematical Modelling, Result and Discussion and Conclusion. Introduction gives an idea of the project why it is important and interesting. It also includes the background of the research, problem statement, research objectives and research scope. Literature review will be focused the fermentation process of ethanol production and the various kinetic models that has been done. The Chapter three will be presented by our two modified models, therefore, this section explains the numerical solutions and parameters estimation of the models. In the chapter four, the simulated result of the models will be discussed. The last chapter includes the findings of the study and projects some future outlooks.

CHAPTER 2

LITERATURE REVIEW

2.1 Introduction

Extensive research has been done to convert lignocellulosic biomass to biofuel through biological process as it has several advantages over chemical process. Bioprocesses are more beneficial from engineering point of view because of their operations at low pressure and temperature, usage of microbial cell as catalyst and requirements of only one purification step rather two steps in chemical process (Salgado et al. 2012). However, some limitations of bioprocess are reported, such as low productivity and yield (Mohamad et al. 2016). Nevertheless, it is plausible to increase the production of biofuels by controlling the variables that affect the metabolism of sugar-consuming yeasts.

The conversion of OPT sap to ethanol comprises a number of physical and chemical changes i.e. pretreatment, enzymatic hydrolysis, and fermentation. The fermentation step converts sugar into ethanol and is an essential part of biomass to ethanol conversion process as shown in Figure 2.1 (Halim 2016). This research focus on the fermentation step and its modelling.

Pretreatment modifies the structure of biomass to make the cellulose more exposed to enzymes for sugar conversion (Himmel et al. 2007). Enzymatic hydrolysis breaks cellulose chains into sugar such as cellobiose and glucose, whereas fermentation process converts sugar into ethanol (Bansal et al. 2009, Griggs et al. 2012a, b).

A number of researchers have studied the influence of process parameters of fermentation to produce ethanol. Investigation of the process parameters (pH, temperature, inoculum level and substrate concentration) are mostly studied in conical flasks (Mohamad et al. 2016, Sampaio et al. 2005). Few fermentation batches were studied in bioreactor with reaction kinetics (Silva et al. 2006, Silva et al. 1996) but the

kinetic modelling of the individual system was not explained. Kinetic modelling is essential for clear understanding of the reaction mechanism to enhance ethanol production and to design the process (Mohamad et al. 2016).

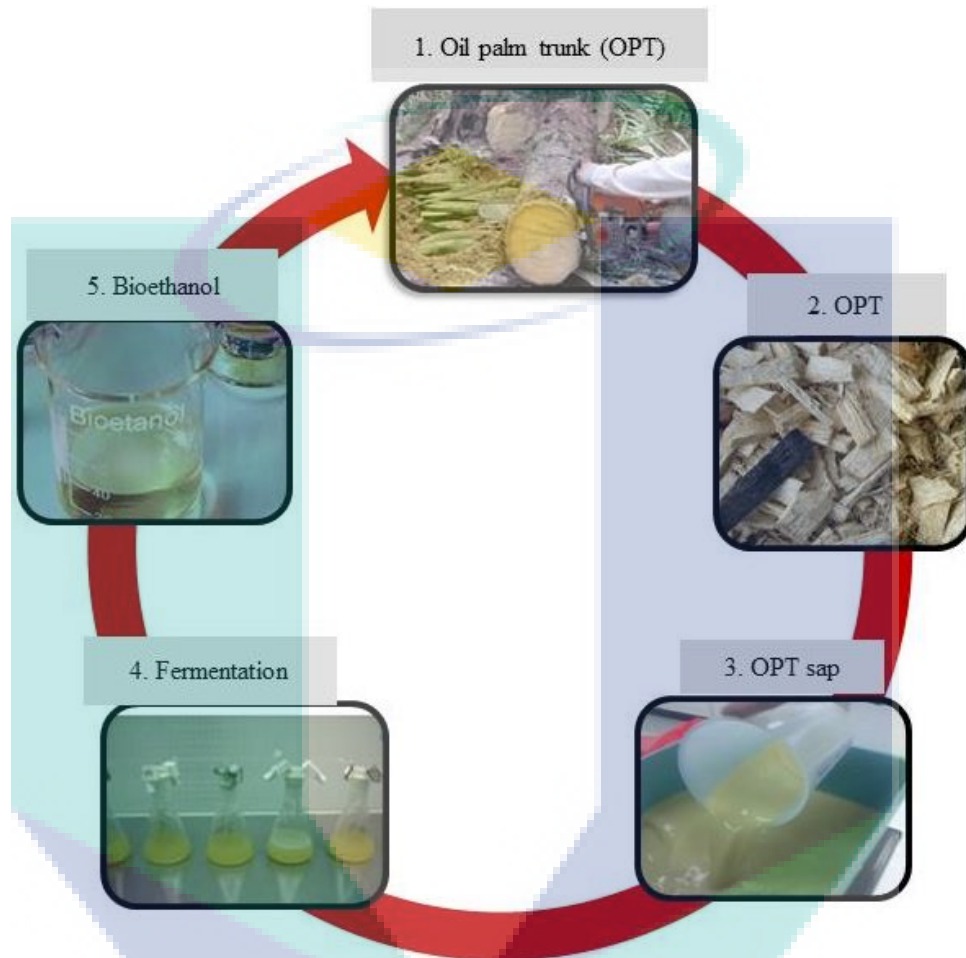


Figure 2.1 Steps of OPT processing to bioethanol

In this chapter, the fermentation process and kinetic modelling are described. It also discusses the theoretical and mathematical developments of the fermentation process studied by Oliveira et al. (2016) and Phisalaphong et al. (2006). Their models are considered as fundamental of our study. An understanding of these models provides a deeper understanding and improving prediction capabilities.

2.2 Fermentation Process

Fermentation is a metabolic process of microorganisms such as bacteria, yeast, fungi, or actinomycete, which converts sugar into amino acids, nucleic acids, enzymes,

organic acids, alcohols and physiologically active substances. Bioethanol can be produced by direct fermentation of sugars, or from other carbohydrates such as starch and cellulose.

The conversion of simple sugars to ethanol and carbon dioxide in the presence of microorganism such as yeasts is called the alcoholic fermentation. Yeast can respire anaerobically and aerobically but it produces ethanol when respiring anaerobically. To date, *Saccharomyce scerevisiae* is considered as most potential microbe to produce bioethanol from OPT sap (Hossain and Jalil 2015, Samsudin and Don 2015). The reaction during ethanol fermentation can be expressed as (Badger 2002)



In the present study, the fermentation was managed at three different temperatures at 25°C, 30°C, and 35°C in static condition. *Saccharomyce scerevisiae* shows it's better performance within the temperature range of 25°C - 35°C basis on the substrate and fermentation conditions (Ona et al. 2019, Phisalaphong et al. 2006). Therefore, experiments were conducted at lower, medium and higher temperature. The initial inoculum size 1.25 g/L and initial sugar 86.63 g/L were used respectively for all temperature as these values were maintained in experiments. Shake flask was purged with nitrogen to remove oxygen to create anaerobic condition. Samples were withdrawn periodically at predetermined time intervals for analysis.

2.3 Kinetic Modeling of Ethanol Fermentation

With increasing interest in the industrial application of fermentation to produce biofuels, various mathematical models of microbial growth have been developed (Fan et al. 2015, Srimachai et al. 2015). It becomes crucial to develop appropriate models for the efficient design of the cell factory for microbial biofuels (Matsuoka and Shimizu 2015). Kinetic models of microbial activities are important tools in explaining properties of the complex biological system (Costa et al. 2016). The mathematical models of fermentation process can be classified as empirical and kinetics. Empirical models are developed from experimental data. They are the recently developed models to use for complex processes and able to coordinate and project large amount of growth

data, however, they are unable to deliver any information regarding cell growth control. On the contrary, kinetic models are established by using the principles of chemistry, physics, and biology.

It is important to have an appropriate model so that it can predict the effect of substrate concentration, substrate inhibition, cell death etc. Kinetic model can lead to a great deal of understanding physical behaviors involving cell growth and providing valuable quantitative information as well (Khalifa 2011).

Research in the area of alcoholic fermentation for microbial growth has followed several approaches. Early work by Monod (1949a) the kinetic model accounts only the factor of substrate limitation through an equation called as Monod's equation. On the other hand, the models of Hinshelwood (1946), Hoppe and Hansford (1982) account only for ethanol inhibition. Other than those factors Aiba and Shoda (1969) also include product inhibition in their model. Ghaly and El-Taweel (1994) was concerned about substrate limitation, substrate inhibition, product inhibition from cheese whey by the yeast *Candida pseudotropicalis*. All of these models were not concerned about the effect of some culture parameters such as temperature, pH and inoculum size. Current literatures in kinetic models of enology (study of wine) have shown that Jin et al. (2012), Kelkar and Dolan (2012); Mohamad et al. (2016) and Oliveira et al. (2016) have proposed on unstructured kinetic models. Specifically Kelkar and Dolan (2012) studied the mutual effect of primary nitrogen concentration and temperature on fermentation and concluded that the yeast cell growth is controlled by nitrogen and sugar concentration. Jin et al. (2012) has applied the Hinshelwood model to explained the roles of preliminary reducing sugar content on the kinetic behaviour of immobilized *Saccharomyces cerevisiae*, where the medium was sweet sorghum stalk juice. They observed that there was a major inhibition on the maximum specific growth rate. However, no significant effect was observed on the maximum specific ethanol production rate with the increase of initial reducing sugar. Mohamad et al. (2016) include limiting effect of xylose (substrate) and oxygen on cell growth and inhibition effect of oxygen on product. Oliveira et al. (2016) accounted the inhibition effect of substrate and product on cell growth but did not consider cell death in their proposed model.

Another essential factor, the effect of temperature was included by Phisalaphong et al. (2006) and Kelkar and Dolan (2012) in their kinetic model. The temperature effect is formulated using the concept of Arrhenius theory. The Arrhenius equation relates the effect of temperature with the reaction rate constant, quantitatively expressed by the empirical equation (Chauhan, 2013) as follows:

$$k = Ae^{-\frac{E}{RT}} \quad 2.1$$

where k is the rate constant, A is the proportionality constant, R is the gas constant, T is the absolute temperature in kelvin, and E is the apparent activation energy for the reaction. In addition, the reaction can also be written as

$$\ln k = -\frac{E}{R}\left(\frac{1}{T}\right) + \ln A \quad 2.2$$

The activation energy can be found by measuring k as a function of temperature. This relationship helps to assess the dependency of kinetic coefficients such as function $k = \{\mu_m\}$ on the temperature under super position of activation energies for cell growth and death. It has the advantage of rapidly assessing the temperature dependence on the growth characteristics. Phisalaphong et al. (2006) has expressed the mathematical model by the Arrhenius equation, where the temperature reliance of the maximum specific growth rate, specific death rate and maximum specific production rate were aligned satisfactorily with the experimental results. Kelkar and Dolan (2012) have applied the Arrhenius relationship to predict the effect of temperature and preliminary nitrogen content on the fermentation kinetics of hard cider.

Some factors that commonly observed in fermentation process are substrate limitation, substrate inhibition, ethanol inhibition, cell death, cell maintenance (Phisalaphong et al. 2006). With regard to these factors, there are three main element in kinetic model for fermentation process, which are:

- a) Cell growth, X
- b) Ethanol production, P
- c) Substrate consumption, S

There are many models that describe cell growth considering different context. Monod equation is one of the significant models because most of the models are developed based on this equation. Monod equation is shown in equation 2.3,

$$\mu = \mu_m \left(\frac{S}{K_s + S} \right) \quad 2.3$$

is widely used to describe the specific cell growth rate. The μ parameter indicates specific growth rate; μ_m refer to maximum cell growth rate; S is substrate concentration; and K_s is saturation constant of substrate (substrate inhibition constant) (Esfahanian et al. 2016). It accounts the decline of cell growth and ethanol production rate because of inhibitory effects (Oliveira et al. 2016). In our model we have applied Monod equation to account the reduction of cell growth, ethanol production and substrate consumption as well. The Monod equation refers to growth rate that increases continually with substrate concentration. Nevertheless, the specific growth rate usually begins to decline above some particular value of S , characterizing by inhibition by substrate.

The substrate inhibition effect is often modelled by Andrew equation (Oliveira et al. 2016) as given by

$$\mu = \hat{\mu} \left(\frac{S}{K_s + S + \frac{S^2}{K_i}} \right) \quad 2.4$$

Generally, several equations describe inhibition by ethanol/product have been proposed, such as (Oliveira et al. 2016)

$$g(P) = \left(1 - \frac{P}{P_m} \right)^n \quad 2.5$$

The important features of the Monod model are that the growth rate will be zero as substrate concentration getting too small ($S \ll K_s$) and when the substrate

concentration is too high ($S \gg K_s$) the specific growth rate will be maximized (Clark and Blanch 1996). The Monod model can be modified based on some assumptions according to each case. For instance, Monod model in Mohamad et al. (2016) includes the concentration of dissolve oxygen and its limiting constant as expressed in Equation 2.6,

$$\mu = \mu_m \left(\frac{S}{S + K_{i,S}} \right) \left(\frac{K_{in,S}}{K_{in,S} + S} \right) \left(\frac{O_2}{O_2 + K_{i,O_2}} \right) \quad 2.6$$

where, $K_{in,S}$ represents the substrate inhibition constant, O_2 is the dissolved oxygen concentration, $K_{i,S}$ is the substrate limitation constant and K_{i,O_2} is the dissolved oxygen limitation constant.

In a model developed by Zhu et al. (2016), cell growth is inhibited by products. Product-inhibited cell growth is usually described by two equations as given below:

$$\mu = \mu_m \left(\frac{S}{K_s + S} \right) \left(\frac{K_p}{K_p + P} \right) \quad 2.7$$

$$\mu = \mu_m \frac{S}{K_s + S} \left[1 - \left(\frac{P}{P^*} \right)^n \right] \quad 2.8$$

where, P is a product (ethanol) concentration; K_p is the inhibition constant of the product; P^* is the critical concentration of product at which cell growth is completely inhibited; and n is a constant. In the model of Phisalaphong et al. (2006), the Monod equation for cell growth is given as

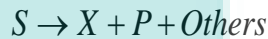
$$\mu = \mu_m \left(\frac{S}{K_s + S + \frac{S^2}{K_{SS}}} \right) \left(1 - \frac{P}{P_M} \right) \quad 2.9$$

Where K_s , K_{ss} , P_M were refer to saturation constant, substrate inhibition and the ethanol inhibition parameter for cell growth.

However, we have choosen Oliviera and Phisalaphong models as base models for this research. Their models are more related to our problem compare to others. Furthermore, both of the models discussed the ethanol fermentation using *Saccharomyces cerevisiae*.

2.4 Kinetic Model by Phisalaphong

According to the Phisalaphong et al. (2006) model, the growth kinetics can be expressed in terms of substrate and product terms combining with death rate and cell maintenance. A simple ethanol fermentation reaction can be stated as follow



(Substrate) \rightarrow (Cell Biomass) + (Product Ethanol) + Others

where S is the substrate concentration, P is the product concentration, and X is the cell concentration. According to the rate of law, the reaction rate for the substrate concentration can be written as

$$r = -\frac{dS}{dt} \tag{2.10}$$

The negative sign indicates that the substrate concentration is decreasing with time t during the fermentation process.

In the fermentation process, the simplest cell growth rate is described as:

$$\frac{dX}{dt} = \mu X \tag{2.11}$$

where, μ is the specific growth rate and X is the cell concentration at fermentation broth. The correlation of specific growth rate μ to substrate concentration S is supposed to form the limiting or saturation kinetics. This kinetics of the fermentation process can be expressed by the Monod equation (Mohamad et al. 2016).

In the Phisalaphong et al. (2006) model, the rate of net cell growth, ethanol production and substrate consumption depend on initial cell, ethanol and substrate concentration.

For cell: net cell growth rate = cell growth rate – cell death rate

$$\frac{dX}{dt} = \mu X - K_d X \quad 2.12$$

For ethanol: ethanol production rate = specific production rate × production concentration

$$\frac{dP}{dt} = \nu P \quad 2.13$$

For substrate: substrate consumption rate = substrate consumed by cell + substrate consumed for ethanol production + substrate consumed for others purpose,

$$-\frac{dS}{dt} = \frac{1}{Y'_{X/S}} \left(\frac{dX}{dt} \right) + \frac{1}{Y'_{P/S}} \left(\frac{dP}{dt} \right) + K_{CM} X \quad 2.14$$

where μ is the specific growth rate, ν is the specific production rate and K_d is the specific death rate representing the rate constants for cell growth, ethanol production and cell death respectively. Parameter K_{CM} represents the maintenance constant. The $Y'_{X/S}$ and $Y'_{P/S}$ parameters represent the yield coefficient for the cell on substrate use for cell formation and the yield coefficient for ethanol on substrate use for ethanol formation respectively.

The μ and ν were controlled by the substrate limiting effect and inhibition effects of the substrate and ethanol as follows:

For μ used the equation (2.9)

$$\nu = \nu_m \left(\frac{S}{K_{SP} + S + \frac{S^2}{K_{SSP}}} \right) \left(1 - \frac{P}{P'_M} \right) \quad 2.15$$

where

ν_m = maximum specific production rate

K_{SP} = saturation constant

K_{SSP} = substrate inhibition term

P'_M = ethanol inhibition term

} for ethanol production

To study the effect of temperature, the following kinetic parameters: μ_m , v_m , K_d , K_S , K_{SS} , P_M , K_{SP} , K_{SSP} , P'_M , $Y'_{X/S}$, $Y'_{P/S}$ and K_{CM} were allowed to fluctuate as a function of the temperature in each experiment. As the model was non-linear with multi-parameters, optimization mainly depend on initial guesses of values of parameters (Phisalaphong et al. 2006).

2.5 Kinetic Model by Oliveira

Some assumptions were given to develop Oliveira's mathematical model (Oliveira et al. 2016) such as

- i) Yeast growth limitation by shortage of substrate;
- ii) Yeast growth inhibition by ethanol and substrate;
- iii) Cell death are not exist.

Based on the above assumptions, the mathematical model for cell growth, ethanol production and substrate consumption are as given below

For Cell: Used the equation (2.11)

For ethanol: $\frac{dP}{dt} = \pi X$

$$\frac{dP}{dt} = \alpha \mu X \quad 2.16$$

For substrate: $\frac{dS}{dt} = -\sigma X$

$$\frac{dS}{dt} = -\frac{\alpha \mu X}{Y'_{P/S}} \quad 2.17$$

where,

$$\mu = \left(\frac{\hat{\mu} S}{K_S + S + \frac{S^2}{K_i}} \right) g(P); \quad 2.18$$

$$\sigma = \frac{\pi}{Y_{P/S}} \quad 2.19$$

$$\pi = \alpha\mu \quad 2.20$$

where $\hat{\mu}$ is the maximum specific growth rate, K_s is the substrate affinity coefficient, $Y_{P/S}$ is the apparent yield coefficient for substrate to ethanol conversion, K_i is the substrate inhibition coefficient, α is the model parameter, P_m is the inhibition parameter for ethanol. The estimated values of $Y_{P/S}$ and α are within the ranges of expected values for alcohol fermentation. To estimate the others parameter, nonlinear regression was used following Marquardt's algorithm to minimize the sum of squared residual (Oliveira et al. 2016).

2.6 Kinetic Model by Leudeking-Piret relationship

Leudeking-Piret (2000) proposed the relationship of product formation to growth rate of microbial biomass considering the factors nutrient concentration, product concentration and cell density at constant temperature. According to this model, the product formation rate depends on both the instantaneous biomass concentration, X and growth rate, $\frac{dX}{dt}$.

$$\frac{dP}{dt} = a \frac{dX}{dt} + bX, \quad 2.21$$

when $a \neq 0, b = 0$, the product formation is associate-growth. The kinetic equations relate quantitatively the rates of product formation to the rates of cell growth and to the cell concentration.

The substrate concentration in Luedeking–Piret equation is used to form cell material and metabolic products as well as the maintenance of cells. The equation is given below

$$\frac{dS}{dt} = -\frac{1}{Y_{X/S}} \left(\frac{dX}{dt} \right) - cX \quad 2.22$$

where c is the coefficient of cell maintenance and $Y_{x/s}$ represents the yield coefficient for the cell on substrate.

2.7 Summary

This chapter reviewed the several proposed kinetic models that describe the cell growth which related to different nutrition or substrate. Oliviera's model did not consider the cell death rate and Phisalaphong's model showed the effect of inhibition effect of substrate and ethanol considering cell death rate but did not discuss any influential effect of cell death rate and initial cell concentration. Leudeking-Piret equation did not discuss the maximum cell growth rate, cell death rate and any inhibition effect. For this reason, considering the effect of the essential factors simultaneously (substrate limitation, substrate inhibition, ethanol inhibition and cell death) our proposed idea believe to be the solutions to the problem identified. Therefore, this chapter gives an idea regarding the influential factors of fermentation process.

The logo of UIMP (Universitas Islam Malang) is a large, stylized letter 'U' shape. The top part of the 'U' is a light blue horizontal bar. The two vertical sides of the 'U' are composed of two overlapping shapes: a light blue one on the left and a light purple one on the right. The bottom part of the 'U' is a light blue inverted triangle. The letters 'UIMP' are written in white, bold, sans-serif font across the center of the bottom part of the 'U'.

CHAPTER 3

MATHEMATICAL MODELLING AND NUMERICAL SOLUTION

3.1 Introduction

This chapter explains in detail two types of kinetic model development denoted by Model I and Model II. The models are expressed by the ordinary differential equation (ODE) associated with yeast cell growth kinetics during fermentation. The ODE relates one or more independent variables and is designed in various context including thermodynamics, physics, mechanics and also population and growth modelling. It is difficult to solve differential equations by analytical method. Therefore, our proposed kinetic models will be solved by 4th order Runge-kutta (RK4) method in MATLAB (version 8.4).

3.2 Model I

This current kinetic models for fermentation process such as Oliveira et al. (2016), Mohamad et al. (2016), Phisalaphong et al. (2006) were studied to modify the kinetic model of cell growth, substrate consumption and ethanol production in terms of cell death rate. Our modified model was then proposed to calculate the numeric linkage between temperature and kinetic behavior of cell.

In order to effectively analyze the kinetics of the fermentation process, we described the ethanol production route and then the phenomenon to express in terms of mathematical equations. The proposed model extends Oliveira's (2016) model by adding cell death rate based on the following assumptions:

- i) Limitation of cell growth due to substrate deficiency;
- ii) Cell growth inhibition by ethanol and substrate;
- iii) Existence of cell death or inactivation.

Cell growth is usually stopped or slows due to the deficiency of substrate concentration. At the same time, cell growth is also inhibited when ethanol concentration is increased. The non-growth cells are considered as death cells which may affects the mass transfer rate of culture broth.

To construct a mathematical model of ethanol fermentation by *Saccharomyces cerevisiae* Kyokai no.7, an extensive kinetic model was used, that was modified from the Monod kinetics (Monod 1949b) to explore the effect of various temperatures. Monod equation 2.3 is used to describe the cell growth and defines the relation between the growth rate and the substrate concentrations. In our proposed model based on Oliveira et al. (2016), the specific growth rate of microorganism, μ was described by the modified Monod equation that includes substrate inhibition and product inhibition as follows by using the Equations 2.5 and 2.18.

$$\mu = \hat{\mu} \frac{S}{K_s + S + \frac{S^2}{K_i}} \left(1 - \frac{P}{P_m}\right)^n, \quad 3.1$$

where P is ethanol concentration, S is substrate concentration, $\hat{\mu}$ is the maximum specific growth rate, K_s is the substrate affinity coefficient, K_i is the inhibition parameter for sugar, and P_m is the inhibition parameter for ethanol.

In model I, the rate of cell growth, ethanol production and substrate consumption were presented by using the equations 2.12, 2.16 and 2.17 as follows

$$\begin{aligned} \frac{dX}{dt} &= \mu X - K_d X, \\ \frac{dP}{dt} &= \alpha \mu X, \\ \frac{dS}{dt} &= -\frac{\alpha}{Y_{p/s}} \mu X. \end{aligned}$$

The $Y_{p/s}$ is the yield coefficient parameter for ethanol on substrate used for ethanol formation, K_d is the cell death rate, α is the model parameter, and n is ethanol toxic

power. The substrate and glucose are required to form a cell material and metabolic products as well as the maintenance of cells (Liu et al. 2003). According to our model, the ethanol production rate depends on instantaneous biomass (cell) concentration, X .

3.3 Model II

This proposed model is based on Phisalaphong et al. (2006) model and Luedeking and Piret (2000) relationship for the solution of substrate consumption and product formation as shown in equation 2.12, 3.2 and 3.3. Model II was modified by the following assumption.

- i) Limitation of cell growth due to substrate deficiency;
- ii) Cell growth inhibition by ethanol and substrate;
- iii) Growth and non-growth associated product formation;
- iv) Existence of cell death or inactivation;
- v) Temperature dependence on cell growth.

$$\begin{aligned} \frac{dX}{dt} &= \mu X - K_d X, \\ \frac{dS}{dt} &= -\frac{1}{Y_{x/s}} \left(\frac{dX}{dt} \right) - cX, \end{aligned} \quad 3.2$$

$$\frac{dP}{dt} = a \frac{dX}{dt} + bX. \quad 3.3$$

From equation 3.1,

$$\mu = \hat{\mu} \left(\frac{S}{K_s + S + \frac{S^2}{K_i}} \right) \left(1 - \frac{P}{P_m} \right)^n$$

where a is growth associated specific productivity coefficient, b is the non-growth associated specific productivity coefficient, c is the coefficient of cell maintenance and $Y_{x/s}$ represents the yield coefficient for the cell on substrate.

Table 3. 1 Summary of mathematical models

	Oliveira et al. (2016)	Proposed model I	Phisalaphong et al. (2006)	Proposed model II
	$\frac{dX}{dt} = \mu X$	$\frac{dX}{dt} = \mu X - K_d X$	$\frac{dX}{dt} = mX - K_d X$	$\frac{dX}{dt} = \mu X - K_d X$
	$\frac{dS}{dt} = -\frac{\alpha}{Y_{P/S}} \mu X$	$\frac{dS}{dt} = -\frac{\alpha}{Y_{P/S}} \mu X$	$\frac{dS}{dt} = -\frac{1}{Y_{X/S}} \left(\frac{dX}{dt}\right) - \frac{1}{Y_{P/S}} \left(\frac{dP}{dt}\right) - K_{CM} X$	$\frac{dS}{dt} = -\frac{1}{Y_{X/S}} \left(\frac{dX}{dt}\right) - cX$
	$\frac{dP}{dt} = \alpha \mu X$	$\frac{dP}{dt} = \alpha \mu X$	$\frac{dP}{dt} = v X$	$\frac{dP}{dt} = a \frac{dX}{dt} + bX$
	$\mu = \hat{\mu} \left(\frac{S}{K_S + S + \frac{S^2}{K_i}} \right) \left(1 - \frac{P}{P_m} \right)^n$	$\mu = \hat{\mu} \left(\frac{S}{K_S + S + \frac{S^2}{K_i}} \right) \left(1 - \frac{P}{P_m} \right)^n$	$\mu = \hat{\mu} \left(\frac{S}{K_S + S + \frac{S^2}{K_i}} \right) \left(1 - \frac{P}{P_m} \right)$	$\mu = \hat{\mu} \left(\frac{S}{K_S + S + \frac{S^2}{K_i}} \right) \left(1 - \frac{P}{P_m} \right)^n$
Cell death rate	No	Yes	Yes	Yes
Temperature dependence (Arrhenius relationship)	No	No	Yes	Yes
Substrate depends on ethanol	Yes	Yes	Yes	Yes

Table 3.1 Continued

	Oliveira et al. (2016)	Proposed model I	Phisalaphong et al. (2006)	Proposed model II
Substrate: Luedeking-Piret	No	No	Yes	Yes
Ethanol - Luedeking-Piret	No	No	No	Yes
Limitation of yeast growth by shortage substrate	Yes	Yes	Yes	Yes
Inhibition of yeast growth by ethanol and substrate	Yes	Yes	Yes	Yes
product formation associated with cell growth	Yes	Yes	Yes	Yes

3.4 Data description

The experimental data of the fermentation process for the bioethanol production from OPT sap by *Saccharomyces cerevisiae* was used in this work. We relied on available data from (Halim 2016). The *Saccharomyces cerevisiae* Kyokai no.7 was used as the microorganism for the production of bioethanol from OPT sap. *Saccharomyces cerevisiae* is well known species for the bioethanol production from sugar based substrate. Moreover, *Saccharomyces cerevisiae* is an attractive model organism due to the fact that its genome has been sequenced, its genetics are easily manipulated, and it is very easy to maintain in the lab. The strain was collected from the Faculty of Engineering Technology, Universiti Malaysia Pahang, Malaysia. Five oil palm trees (26 years old) felled for replantation purposes were freshly obtained from a plantation in Negeri Sembilan, Malaysia. The upper part of the oil palm that contains fruit and frond was removed together with the root. Next, OPT (10 m) was cut into several small pieces to undergo squeezing process by using sugar cane press machine (Robin brand, 5 HP) to obtain the liquid sap. The full process of OPT sap preparation and its fermentation procedure is summarized in Figure 3.1(Halim 2016).

OPT sap was collected in a big container and mixed well before divided into 5 L bottle-shaped reactor. It was kept under -20°C for storage. OPT sap was mixed well in a container before storage since different part of OPT gain different compositions of sugar. OPT sap media was filtered with $9.0\ \mu\text{m}$ filter prior to use. The composition of OPT sap at different part of trunks was also checked.

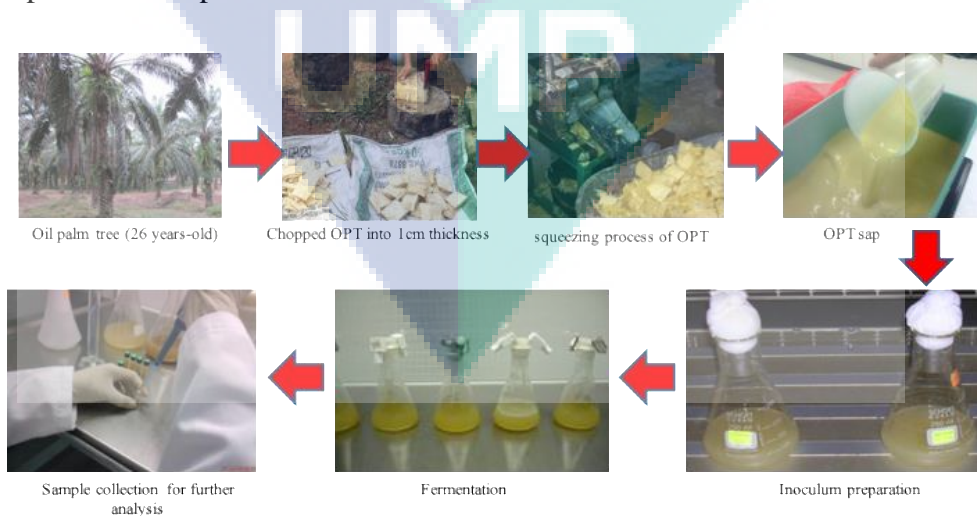


Figure 3.1 OPT sap preparation and fermentation

During the fermentation period, 2 ml sample was taken at each time interval using a disposable syringe (5ml) and centrifuged at 10000 rpm/ 11963 g force for 5 mins to separate the supernatant from the pellet using microcentrifuge (Biofuge Pico, Heraeus). After supernatant was removed, and pellet was dissolved in distilled water for rinsing, cell growth was monitored by measuring optical density of the dissolved pellet at 600 nm (OD 600) using an UV-VIS spectrophotometer (Hitachi U-1800 Spectrophotometer). Distilled water was used as a reference. For cell, dry weight (CDW) determination, the pellets were dried in a 60°C oven until they reached constant weight. All CDW determination was repeated (3-5 times) for consistency.

Sugar concentration was determined by High Performance Liquid Chromatography (HPLC) with refractive index (RI) detector (Agilent Carbohydrate Analysis Column) maintaining the ratio of acetonitrile to water 4:1 and flow rate of 1.4 ml/min. Volume of injected sample was 10.0 µl and temperature was maintained at 60°C for column. The solvent used for washing and dilution was ultrapure water.

Gas chromatography (Agilent Technologies 6890 Series) equipped with a flame ionization detector (FID) was used to determine bioethanol concentrations. The column was HP-INNOWax Polyethylene Glycol (30 m x 250 µm x 0.25 µm nominal). Initial temperature, maximum temperature, and temperature rate in the oven were 50°C, 170°C and 20°C/min, respectively. Temperature of injector and detector were set at 250°C. Helium was used as carrier gas at a flow rate of 45 ml/min.

The value was measured as “peak area” which was then converted into ethanol concentration (g/l) using a standard curve. The n-propanol was used for washing and dilution. One part of sample was mixed with 9 part of n-propanol and was filtered through 0.2-micron nylon membrane (Fisher Scientific™).

3.5 Numerical solution

In this study, Model I and Model II are simulated using numerical approximation scheme. Numerical approximation implements algorithms for obtaining the approximate solutions of the problem. Different numerical methods are used to solve the kinetic model of fermentation processes. Zhu et al. (2016), Oliveira et al. (2016) and Kelkar and Dolan (2012) applied 4th order Runge-Kutta method to solve the kinetic model of microbial growth for ethanol fermentation. Some other researchers

(Bosse and Griewank 2014, Tian et al. 2014) used Euler method for fermentation process. In our analysis (X, P, S) are the dependent variables and were calculated at any time (t) by series of small steps from the initial values and were solved using the MATLAB (version 8.4). The ordinary differential equations in our model I and II will be solved numerically by the (RK4) Method.

3.6 Runge-Kutta method

The Runge-Kutta methods are a family of implicit and explicit iterative methods in numerical analysis. It includes the Euler Method, used in temporal discretization for the approximate solution of ordinary differential equations (ODE). We choose (RK4) method, because it is an effective and widely used method for solving the initial-value problems of differential equations. Runge–Kutta method can be used to construct high order accurate numerical method by functions' self without needing the high order derivatives of functions (Zheng and Zhang 2017). The most popular RK methods are fourth order and for solving a system of ODE is formulated as

$$\begin{aligned}x_{i+1} &= x_i + \frac{h}{6}(k_1 + 2k_2 + 2k_3 + k_4), \\y_{i+1} &= y_i + \frac{h}{6}(k_1 + 2k_2 + 2k_3 + k_4), \\z_{i+1} &= z_i + \frac{h}{6}(k_1 + 2k_2 + 2k_3 + k_4), \\t_{i+1} &= t_i + h,\end{aligned}$$

where,

$$\begin{aligned}k_{x,1} &= f_1(t_i, x_i, y_i, z_i) \\k_{y,1} &= f_2(t_i, x_i, y_i, z_i) \\k_{z,1} &= f_3(t_i, x_i, y_i, z_i)\end{aligned}$$

$$k_{x,2} = f_1 \left(t_i + \frac{h}{2}, x_i + \frac{k_{x,1}}{2} h, y_i + \frac{k_{y,1}}{2} h, z_i + \frac{k_{z,1}}{2} h \right)$$

$$k_{y,2} = f_2 \left(t_i + \frac{h}{2}, x_i + \frac{k_{x,1}}{2} h, y_i + \frac{k_{y,1}}{2} h, z_i + \frac{k_{z,1}}{2} h \right)$$

$$k_{z,2} = f_3 \left(t_i + \frac{h}{2}, x_i + \frac{k_{x,1}}{2} h, y_i + \frac{k_{y,1}}{2} h, z_i + \frac{k_{z,1}}{2} h \right)$$

$$k_{x,3} = f_1 \left(t_i + \frac{h}{2}, x_i + \frac{k_{x,2}}{2} h, y_i + \frac{k_{y,2}}{2} h, z_i + \frac{k_{z,2}}{2} h \right)$$

$$k_{y,3} = f_2 \left(t_i + \frac{h}{2}, x_i + \frac{k_{x,2}}{2} h, y_i + \frac{k_{y,2}}{2} h, z_i + \frac{k_{z,2}}{2} h \right)$$

$$k_{z,3} = f_3 \left(t_i + \frac{h}{2}, x_i + \frac{k_{x,2}}{2} h, y_i + \frac{k_{y,2}}{2} h, z_i + \frac{k_{z,2}}{2} h \right)$$

$$k_{x,4} = f_1 \left(t_i + h, x_i + k_{x,3} h, y_i + k_{y,3} h, z_i + k_{z,3} h \right)$$

$$k_{y,4} = f_2 \left(t_i + h, x_i + k_{x,3} h, y_i + k_{y,3} h, z_i + k_{z,3} h \right)$$

$$k_{z,4} = f_3 \left(t_i + h, x_i + k_{x,3} h, y_i + k_{y,3} h, z_i + k_{z,3} h \right).$$

3.6.1 Model I

Model I is solved numerically by a RK4 scheme with step size of 1 implemented in Matlab (Appendix A).

Step 1: Identify

$$f_1(t_i, X_i, P_i, S_i) = \left(\frac{\hat{\mu} X_i S_i}{K_S + S_i + \frac{S_i^2}{K_i}} \right) \left(1 - \frac{P_i}{P_m} \right)^n - K_d X_i$$

$$f_2(t_i, X_i, P_i, S_i) = \left(\frac{\alpha \hat{\mu} X_i S_i}{K_S + S_i + \frac{S_i^2}{K_i}} \right) \left(1 - \frac{P_i}{P_m} \right)^n$$

$$f_3(t_i, X_i, P_i, S_i) = -\frac{1}{Y_{P/S}} \left(\frac{\alpha \hat{\mu} X_i S_i}{K_S + S_i + \frac{S_i^2}{K_i}} \right) \left(1 - \frac{P_i}{P_m} \right)^n$$

with initial values $X_0 = 1.25$, $S_0 = 86.63$ over the interval $0 \leq t \leq 50$ with a step size, $h = 1$.

Step 2: Do iterations

$$\begin{aligned}
 k_{X,1} &= f_1(t_i, X_i, P_i, S_i) \\
 k_{P,1} &= f_2(t_i, X_i, P_i, S_i) \\
 k_{S,1} &= f_3(t_i, X_i, P_i, S_i) \\
 k_{X,2} &= f_1\left(t_i + \frac{h}{2}, X_i + \frac{k_{X,1}}{2}h, P_i + \frac{k_{P,1}}{2}h, S_i + \frac{k_{S,1}}{2}h\right) \\
 k_{P,2} &= f_2\left(t_i + \frac{h}{2}, X_i + \frac{k_{X,1}}{2}h, P_i + \frac{k_{P,1}}{2}h, S_i + \frac{k_{S,1}}{2}h\right) \\
 k_{S,2} &= f_3\left(t_i + \frac{h}{2}, X_i + \frac{k_{X,1}}{2}h, P_i + \frac{k_{P,1}}{2}h, S_i + \frac{k_{S,1}}{2}h\right) \\
 k_{X,3} &= f_1\left(t_i + \frac{h}{2}, X_i + \frac{k_{X,2}}{2}h, P_i + \frac{k_{P,2}}{2}h, S_i + \frac{k_{S,2}}{2}h\right) \\
 k_{P,3} &= f_2\left(t_i + \frac{h}{2}, X_i + \frac{k_{X,2}}{2}h, P_i + \frac{k_{P,2}}{2}h, S_i + \frac{k_{S,2}}{2}h\right) \\
 k_{S,3} &= f_3\left(t_i + \frac{h}{2}, X_i + \frac{k_{X,2}}{2}h, P_i + \frac{k_{P,2}}{2}h, S_i + \frac{k_{S,2}}{2}h\right) \\
 k_{X,4} &= f_1(t_i + h, X_i + k_{X,3}h, P_i + k_{P,3}h, S_i + k_{S,3}h) \\
 k_{P,4} &= f_2(t_i + h, X_i + k_{X,3}h, P_i + k_{P,3}h, S_i + k_{S,3}h) \\
 k_{S,4} &= f_3(t_i + h, X_i + k_{X,3}h, P_i + k_{P,3}h, S_i + k_{S,3}h)
 \end{aligned}$$

Therefore

$$\begin{aligned}
 X_{i+1} &= X_i + \frac{h}{6}(k_{X,1} + 2k_{X,2} + 2k_{X,3} + k_{X,4}) \\
 P_{i+1} &= P_i + \frac{h}{6}(k_{P,1} + 2k_{P,2} + 2k_{P,3} + k_{P,4}) \\
 S_{i+1} &= S_i + \frac{h}{6}(k_{S,1} + 2k_{S,2} + 2k_{S,3} + k_{S,4}) \\
 t_{i+1} &= t_i + h
 \end{aligned}$$

3.6.2 Model II

RK4 scheme is used to solve Model II.

Step 1: Identify

$$f_2(t_i, X_i, P_i, S_i) = a \left(\left(\frac{\hat{\mu} X_i S_i}{K_s + S_i + \frac{S_i^2}{K_i}} \left(1 - \frac{P_i}{P_m} \right)^n - K_d X_i \right) + b X_i \right)$$

$$f_3(t_i, X_i, P_i, S_i) = -\frac{1}{Y_{X/S}} \left(\left(\frac{\hat{\mu} X_i S_i}{K_s + S_i + \frac{S_i^2}{K_i}} \left(1 - \frac{P_i}{P_m} \right)^n - K_d X_i \right) - c X_i \right)$$

with initial values $X_0 = 1.25$, $S_0 = 86.63$ over the interval $0 \leq t \leq 50$ with a step size, $h = 1$.

Step 2: Do iterations

$$k_{X,1} = f_1\left(t_i, X_i, P_i, S_i\right)$$

$$k_{P,1} = f_2\left(t_i, X_i, P_i, S_i\right)$$

$$k_{S,1} = f_3\left(t_i, X_i, P_i, S_i\right)$$

$$k_{X,2} = f_1\left(t_i + \frac{h}{2}, X_i + \frac{k_{X,1}}{2}h, P_i + \frac{k_{P,1}}{2}h, S_i + \frac{k_{S,1}}{2}h\right)$$

$$k_{P,2} = f_2\left(t_i + \frac{h}{2}, X_i + \frac{k_{X,1}}{2}h, P_i + \frac{k_{P,1}}{2}h, S_i + \frac{k_{S,1}}{2}h\right)$$

$$k_{S,2} = f_3\left(t_i + \frac{h}{2}, X_i + \frac{k_{X,1}}{2}h, P_i + \frac{k_{P,1}}{2}h, S_i + \frac{k_{S,1}}{2}h\right)$$

$$k_{X,3} = f_1\left(t_i + \frac{h}{2}, X_i + \frac{k_{X,2}}{2}h, P_i + \frac{k_{P,2}}{2}h, S_i + \frac{k_{S,2}}{2}h\right)$$

$$k_{P,3} = f_2\left(t_i + \frac{h}{2}, X_i + \frac{k_{X,2}}{2}h, P_i + \frac{k_{P,2}}{2}h, S_i + \frac{k_{S,2}}{2}h\right)$$

$$k_{S,3} = f_3\left(t_i + \frac{h}{2}, X_i + \frac{k_{X,2}}{2}h, P_i + \frac{k_{P,2}}{2}h, S_i + \frac{k_{S,2}}{2}h\right)$$

$$\begin{aligned}
k_{X,4} &= f_1(t_i + h, X_i + k_{X,3}h, P_i + k_{P,3}h, S_i + k_{S,3}h) \\
k_{P,4} &= f_2(t_i + h, X_i + k_{X,3}h, P_i + k_{P,3}h, S_i + k_{S,3}h) \\
k_{S,4} &= f_3(t_i + h, X_i + k_{X,3}h, P_i + k_{P,3}h, S_i + k_{S,3}h)
\end{aligned}$$

Therefore,

$$\begin{aligned}
X_{i+1} &= X_i + \frac{h}{6}(k_{X,1} + 2k_{X,2} + 2k_{X,3} + k_{X,4}) \\
P_{i+1} &= P_i + \frac{h}{6}(k_{P,1} + 2k_{P,2} + 2k_{P,3} + k_{P,4}) \\
S_{i+1} &= S_i + \frac{h}{6}(k_{S,1} + 2k_{S,2} + 2k_{S,3} + k_{S,4}) \\
t_{i+1} &= t_i + h
\end{aligned}$$

Model I and II have been solved numerically by RK4 scheme with step size of 1 using in Matlab software (Appendix B). In model I and II, the initial values for (X, P, S) were taken from population distributions derived from the available data. We started the model by adjusting manually the parameter values to obtain a good fit to the experimental data. The parameters in the model are varies to compare the effect of various temperatures. To obtain best fit values, the model parameters were estimated using the least square method to minimize the objective function, $f_{objective}$ as shown below:

$$f_{objective} = \sum_{i=1}^n [f(x_i) - y_i]^2 \quad 3.5$$

where $f(x_i)$ is the calculated data and y_i is the experimental data.

3.7 Parameter estimation

The estimation of fermentation parameters becomes crucial part in the authentication and consequential use of a mathematical model (Wang and Sheu 2000). The system of equations consists more than one parameter. Some parameters may be derived from theory or measured directly. However, there are parameters that cannot be

determined by either of these approaches. To estimate the unknown parameters in the system, we compare the equations with the experimental data. In this approach, we can systematically vary the parameters so that we can get the minimum difference between the solution of differential equations and the data.

There are two elements involved for estimating model parameters from data.

- i) First, we need to construct an error function that measures the difference between a model with a certain parameter and the data.
- ii) Second, we need an optimization method that iteratively finds the value of parameter that minimizes the error.

Some examples of minimization algorithm are Nelder-Mead simplex method and Lavenberg-Marquardt method. Some stochastic search algorithms are simulated annealing, Markov Chain Monte Carlo or genetic algorithm. The most common choice for the error function is by using the least squares error scheme (Beale et al. 2010):

$$E_D(\alpha) = \sum_{i=1}^n \|u(t_i) - x(t_i)\|^2 \quad 3.6$$

where $u(t_i)$ is the calculated data, $x(t_i)$ is the experimental data. As measurement errors are normally distributed, independently the error function becomes the logarithm of the likelihood of the data ($\log(\text{likelihood})$). Minimizing the error function is equivalent to maximum likelihood estimation of the parameters.

3.7.1 Nelder-Mead simplex algorithm

By implementing Runge-Kutta algorithm in Matlab and a Nelder-Mead simplex method as an optimization routine for unknown parameter estimation. Nelder-Mead algorithm is a built in Matlab program which minimizes a scalar function of several variables. It is widely used to solve parameter estimation, where the function values are uncertain or subject to noise. The algorithm is dynamic due to its very tolerant of noise in the function values. Therefore, it need not be computed exactly and there is a

possibility to obtain an approximate function value using many fewer floating point computations. Fminsearch is applied in Matlab to find the minimum of a scalar function of several variables.

3.8 Flow chart of numerical solution

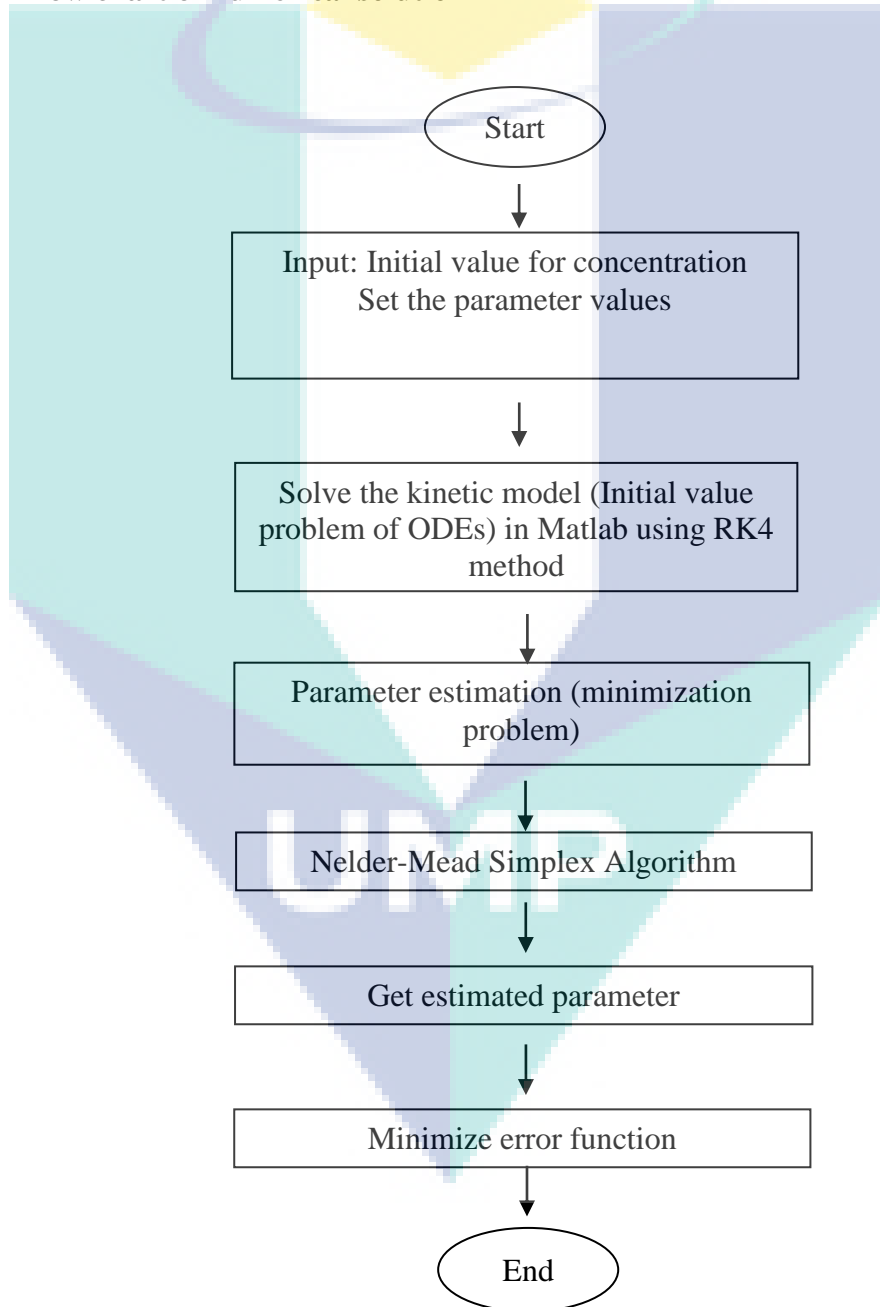
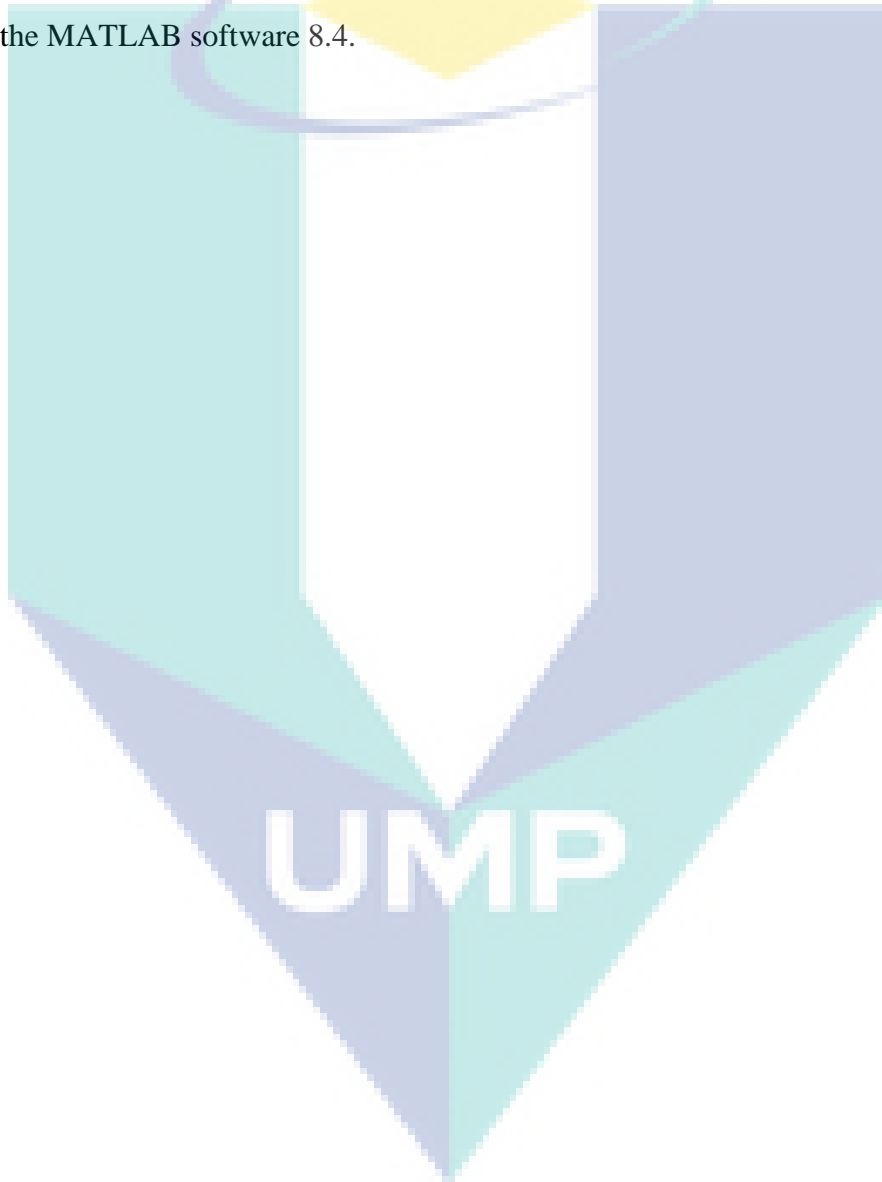


Figure 3.2 Flow chart of numerical solution

3.9 Summary

In this chapter, two types of model based on the typical model structure are modified. The considering parameters, basic models and our proposed models are summarised in Table 3.1. To investigate the effect of cell death rate, Oliviera's (2016) model is extended by adding cell death rate in model I. The model II is the modification of Oliviera (2016) and Phisalaphong (2006) model with Leudeking-Piret relationship (2000). The ordinary differential equations of these models are solved numerically by using the MATLAB software 8.4.



CHAPTER 4

RESULTS AND DISCUSSION

4.1 Introduction

In this work, two models are proposed for fermentation process of OPT sap, namely - Model I and Model II. The Model I is an extension from Oliveira's (2016) model by adding cell death rate term only. On the other hand, Model II is a modification from Oliveira and Phisalaphong (2006) model with the Luedeking–Piret (2000) equations for substrate consumption and ethanol production. Model II includes all factors, such as are cell death rate and temperature depends on kinetic parameters and Luedeking–Piret equations for substrate consumption and ethanol production.

In this chapter, the results of two sets of simulation are presented and discussed. First, the effect of cell death rate during ethanol fermentation from OPT sap in Model I is simulated and the result is compared with the experimental data of Oliveira's model. Next, the Luedeking–Piret equations for substrate consumption and ethanol production together with the effects of temperature on the kinetic parameters of Model II is assessed. In addition, cell death rate is also simulated and discussed. The aim of this chapter is to illustrate the kinetic model of fermentation process that include cell death rate and temperature dependence. In addition, the validity by fitting with the experimental data comparing to Oliveira and Phisalaphong model are also justified.

4.2 Model I: Simulated result

Experimental data (batch fermentation) were used to estimate the unknown parameters of the proposed models in Equations 2.12, 2.16 and 2.17. The initial values of sugar and cell concentration were obtained from the experimental results with average values of $S(0) = 86.63\text{g}/L$, $X(0) = 1.25\text{g}/L$ respectively and the inhibition

parameter for ethanol, P_m also obtained from the experimental results for different temperatures. The values of initial parameter $\hat{\mu}, K_d, K_s, K_i, Y_{p/s}, \alpha, n$ were tentatively predicted by manual adjustment to obtain a good fit to the experimental data. Next, the initial estimates of kinetic parameters were re-calculated by running the program iterations.

Table 4.1 Values of the kinetic parameters at different temperature estimated by nonlinear regression

Parameter	Notation	Estimated value		
		25°C	30°C	35°C
Maximum specific growth rate (h^{-1})	$\hat{\mu}$	1.1680	0.5779	0.5787
Substrate inhibition constant for cell growth (g/L)	K_s	0.0397	0.0277	0.0956
Specific cell death rate (h^{-1})	K_d	0.0001	0.0068	-0.0072
Apparent yield coefficient for substrate to ethanol conversion	$Y_{p/s}$	0.6520	0.5836	0.5986
Inhibition parameter for sugar (g/L)	K_i	26.1107	183.4506	49.6145
Inhibition parameter for ethanol (g/L)	P_m	29.9024	30.7600	26.0600
Model parameter (g/g)	α	0.7872	0.5672	0.8459
Ethanol toxic power	n	1.7432	1.6530	1.8930

The best-fit values of the parameter were determined by the least-squares method based on nonlinear regression function performed in MATLAB. Table 4.1 displays the estimated values of the parameters which were obtained from the model. Analysing the data in Table 4.1, the maximum value of $\hat{\mu}$ is obtained at 25°C which is in agreement with findings ($1.08h^{-1}$) of Garnier and Gaillet (2015). Due to the inhibition effect of substrate on cell growth at this temperature, the result could change the metabolic activity in the cells. This phenomenon might increase the accumulation of toxic concentration including ethanol inside the cells. The lowest value of K_s occurred at 30°C reveals a high attraction of the microorganism for the substrate utilization. The parameter, ethanol toxic power (n) shows strong inhibition on the cell growth by

ethanol or the yeast cell shows a very low tolerance to ethanol when the parameter value is high (Oliveira et al. 2016). Our model reveals that, the values of ethanol toxic power almost constant. However, the lowest value was observed at 30°C and the highest value of $n=1.8930$ at 35°C. As compared to the Oliveira's model, both of the values are lower, meanings that low inhibition of the cell growth was present in the system. The estimated values of ethanol yield $Y_{P/S}$, are closer to the values reported by Guidini et al. (2014). Although the highest ethanol yield was observed at 25°C, the inhibition parameter for sugar ($K_i=183.4506$) was higher at 30°C, indicates that the ethanol was inhibited by the substrate after that level of concentration. Therefore, the ethanol inhibition parameter value or the product concentration, $P_m=30.7600$ was maximum at 30°C and later cell growth start to terminate. It is suggested that ethanol production is highly affected by temperature and the most suitable temperature is 30°C.

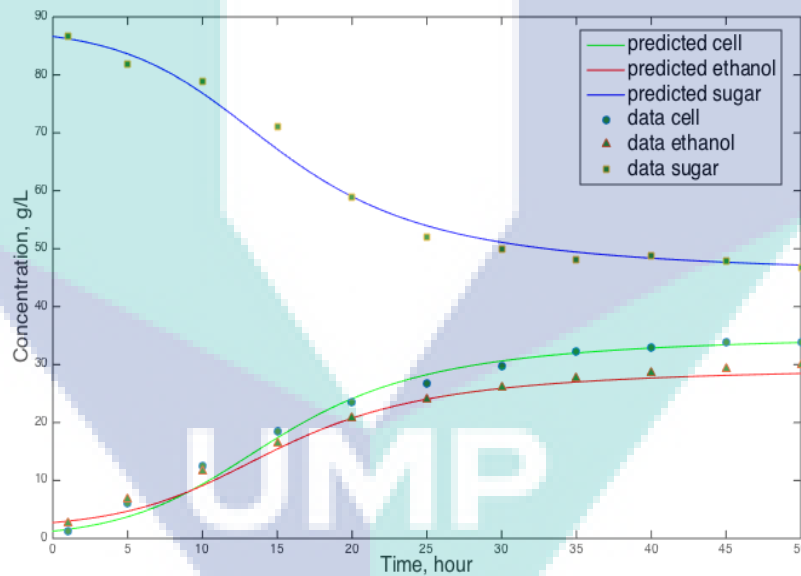


Figure 4.1 Experimental data and model predictions of batch fermentation at 25°C temperature

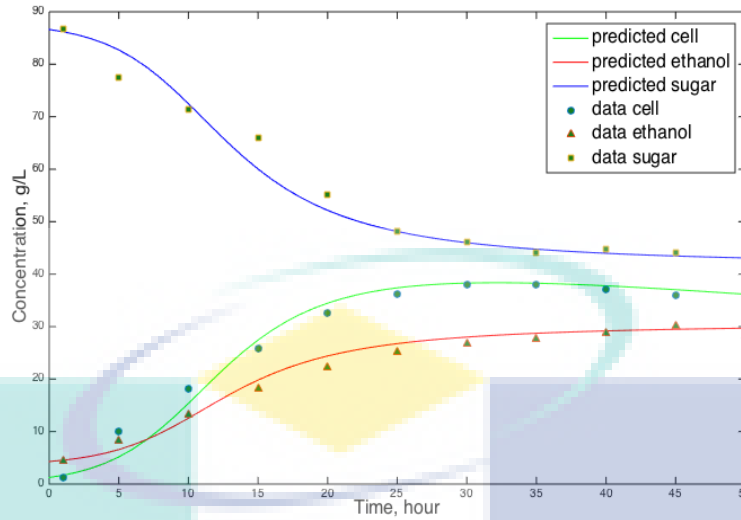


Figure 4.2 Experimental data and model predictions of batch cultivations at 30°C temperature

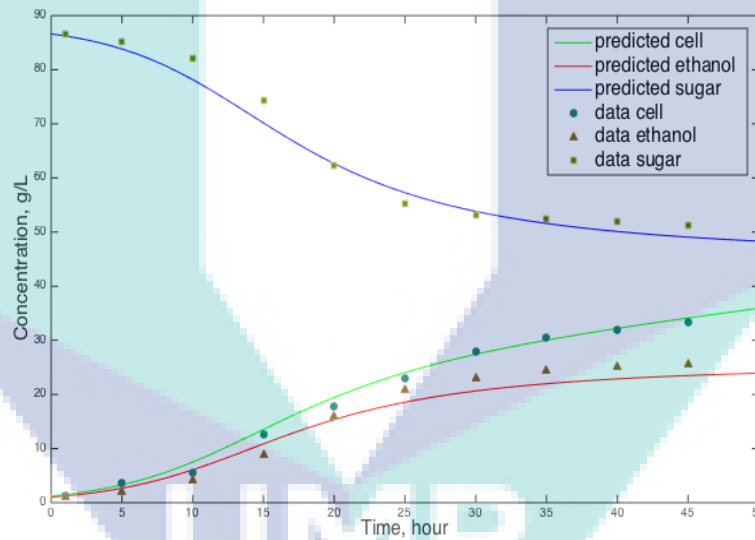


Figure 4.3 Experimental data and model predictions of batch cultivations at 35°C temperature

Figure 4.1-4.3 show the concentration profiles of cell, sugar, and ethanol of the fermentation process which demonstrate a good agreement between experimental data and the simulation results of the temperatures 25°C, 30°C, and 35°C, respectively. The simulated results also show that the sugar concentration diminished monotonically with time until its full depletion, while cell and product concentrations increased monotonically until a stationary phase was attained. The ethanol fermentation by *Saccharomyces cerevisiae* shows a classical growth trend. After a lag phase (about 1-2

h), the cells entered an exponential growth phase and then the cell growth and the ethanol production took place simultaneously. From the result, it can be seen that the ethanol production has strong linear relationship with the cell growth.

According to these Figures, model predictions (lines) agree with the experimental data (circles, triangles, squares) qualitatively. The results of the Model I and the experimental data consistently interpreted that the predicted models give a satisfactory fit to the experimental data for all temperature to reproduce the profiles of all the three bioprocess variables throughout the fermentation process. Therefore, Model I and estimated kinetic parameters developed from the small scale could adequately predict the dynamics of ethanol fermentation in 10 litre fermenter. Table 4.2 shows the Relative Root Mean Squared Error (rRMSE) analysis at different temperature for sugar, cell, and ethanol profiles, which was used for model accuracy. This table shows the comparison between our proposed model (Model I) and Oliveira's model. The values are the means with the corresponding of confidence intervals (95%). The rRMSE was calculated based on the equation 4.1:

$$rRMSE = 100 \times \frac{1}{A} \sqrt{\frac{1}{n} \sum_{r=1}^n (O_r - P_r)^2} \quad 4.1$$

where A is the average observed value, n is the number of samples, O_r is the observed value of profile r and P_r is the predicted value of the profile r .

Table 4. 2 Comparison of relative root mean squared error (rRMSE) for accuracy of the proposed model (Model I) with Oliveira's model

Profile	rRMSE (%)					
	For Oliveira's model			Model I		
Temperature	25 °C	30 °C	35 °C	25 °C	30 °C	35 °C
Cell (X)	3.6520	35.5699	34.3893	8.3032	9.2128	4.4427
Sugar (S)	5.5635	10.2946	14.0975	2.7230	5.0585	2.9307
Ethanol (P)	44.9484	22.8361	4.3297	8.3312	6.1069	12.6278

The rRMSE value lower than 15% indicates the good prediction of the model (Talib et al. 2014). In the proposed model, for all temperatures, there is a good agreement between the measured and predicted data where rRMSE values lay between

2.7230% and 12.6278% for the cell growth, ethanol production and substrate consumption. This result has been predicted with the consideration of cell death rate. On the other hand, Oliveira et al. (2016) did not consider the cell death rate and reported that the higher rRMSE values at the range of 3.6520% to 44.9484% indicating poor prediction of the model. Therefore, it could be concluded that cell death rate has a very significant influence on the mathematical study of the ethanol production through fermentation process.

4.3 Model II: Simulated result

We have modified a relatively simple model in which the effect of temperature on yeast growth rates is incorporated into a substrate consumption and product expansion of the Leudeking-Piret model. With this new model, the combined effects of temperature and substrate limitation can be described. To estimate the unknown parameters for the proposed Model II, Equations 3.1, 3.4 and 3.5 are used and for the initial conditions, the sugar and cell concentration are maintained at $S(0) = 86.63 \text{ g/L}$, $X(0) = 1.25 \text{ g/L}$ for different temperature. In model II, the unknown parameters such as $\hat{\mu}$, K_d , K_i , K_s , $Y_{x/s}$, a , b , c , n are predicted by manual adjustment to the experimental data.

The higher temperature could inhibit the mass transfer of soluble compounds and solvent within the cells that might causes the accumulation of toxic components including ethanol inside the cell compartments. The numerical value of sugar inhibition constant K_s reflects the microorganism's affinity to its substrate and the K_s value is reversely proportional to affinity (Papagianni et al. 2007). According to the Table 4.3, a high attraction of the microorganism to the substrate was observed when K_s value was lowest at 30°C. Furthermore, at 30°C, when the inhibition parameter for sugar was $K_i = 290.4042$, ethanol inhibition was started by the substrate concentration. Similar phenomenon was found for Model I and therefore, the ethanol inhibition parameter value $P_m = 30.76$ were the highest at 30°C. The estimated value of K_i for the Model II is greater than Model I, that implies cell viability is longer in the Model II. With the increase of temperature from 25°C to 35°C the maximum specific growth rate ($\hat{\mu}$) was decreased from 1.5845 to 0.5065 as shown in Table 4.3, which indicated that cell

growth was inhibited at high temperature. However, from the overall discussion and parameter analysis, it can be concluded that 30°C is the suitable temperature for ethanol production from the OPT sap based on the experimental data (Halim 2016).

Table 4.3 Values of the kinetic parameters at different temperature estimated by nonlinear regression

Parameter	Notation	Estimated value		
		25°C	30°C	35°C
Maximum specific growth rate (h ⁻¹)	$\hat{\mu}$	1.5845	0.7821	0.5065
Substrate inhibition constant for cell growth (g/L)	K_s	5.2053	1.3832	8.7677
Specific cell death rate (h ⁻¹)	K_d	-0.0079	0.0005	-0.0117
Apparent yield coefficient for the cell on substrate	$Y_{x/s}$	0.8918	1.1250	0.7308
Inhibition parameter for sugar (g/L)	K_i	27.0843	290.4042	71.2317
Inhibition parameter for ethanol (g/L)	P_m	29.9024	30.7600	26.0600
Ethanol toxic power	n	3.00	3.00	3.00
Growth associated specific productivity coefficient	a	0.6184	0.4414	0.4475
Non-growth associated specific productivity coefficient	b	0.0072	0.0075	0.0140
Coefficient of cell maintenance	c	0.0037	0.0097	-0.0087

The temperature dependency on cell growth rate can be established by means of Arrhenius equation (equation 2.2). By the illustration of Arrhenius relationship, the temperature dependency of the cell growth rate was fitted very well with the experimental results as shown in Figure 4.4.

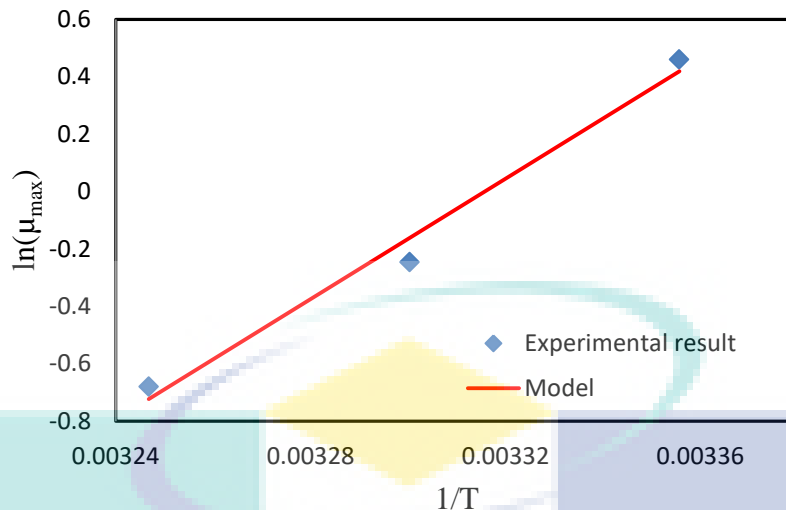


Figure 4.4 Arrhenius plots illustrating the effect of temperature on (a) the maximum specific growth rate (μ_{\max})

Based on the Figure 4.4, the estimated values of the activation energy (E) for cell growth is -82.56 KJ/mol, which indicates the barrier less growth environment for the bioethanol production from OPT sap by the *Saccharomyce scerevisiae*.

Figure 4.5-4.7 explain the experimental results, as well as the modelled values of the fermentation profile at different temperature with the same initial cell and sugar concentration of 1.25 g/L and 86.63 g/L respectively. According to these Figures, substrate concentration was reduced monotonically until its full reduction, whereas cell and product concentration were increased monotonically prior to reach to the stationary phase. As illustrated in those Figures (4.5-4.7), the predicted models finely fitted to the experimental data for the cell, ethanol and substrate concentration at 30°C from the beginning up to the stationary phase. But for the 35°C , model fitting was slightly deviated for ethanol due to the inconsistency of the cell growth at high temperature. Biomass increased exponentially at the beginning and entered a stationary phase after approximately 35 hour. However, the trend of the predicted model is acceptable for the temperature range 25° to 35°C , since it clearly presents lag, exponential and stationary phases. To increase the accuracy of the model, the parameter estimation function should depends on temperature (Rivera et al. 2016). From the result, it can be seen that ethanol formation is strongly linearly related to the cell growth. Based on the value of a and b from Table 4.3, the production of ethanol is growth associated at 25°C and 30°C , and that is non-growth-associated at 35°C Figures 4.5-4.7 (Garnier and Gaillet 2015).

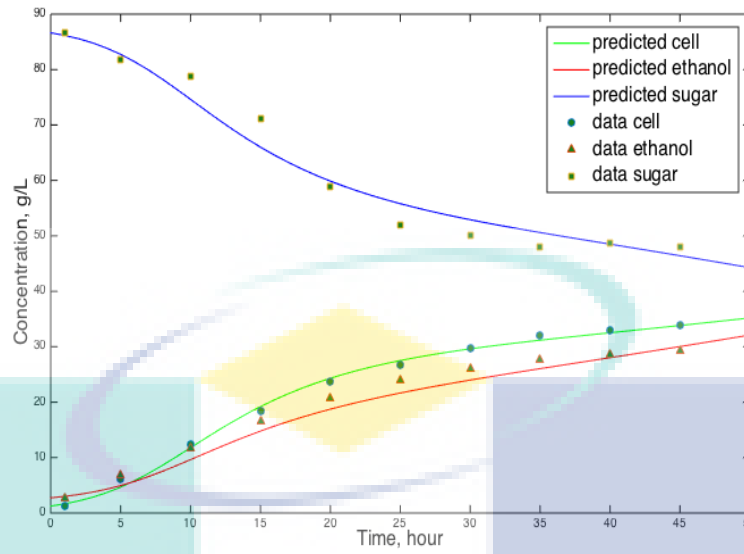


Figure 4.5 Experimental data and model predictions of batch fermentation at 25°C temperature

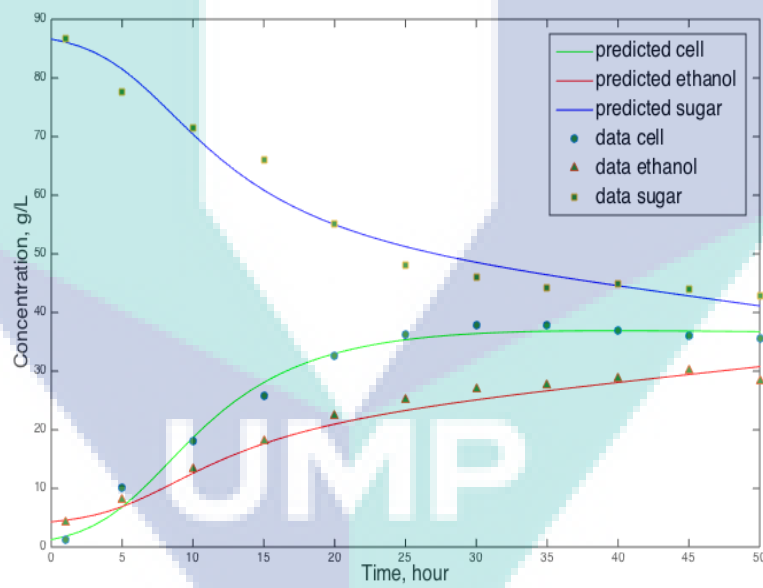


Figure 4.6 Experimental data and model predictions of batch fermentation at 30°C temperature

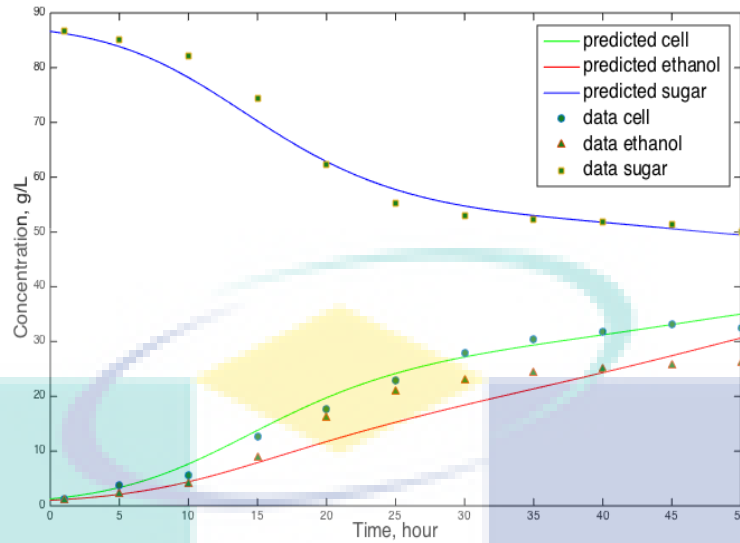


Figure 4.7 Experimental data and model predictions of batch fermentation at 35°C temperature

Table 4.4 shows the Relative Root Mean Squared Error (rRMSE) analysis at different temperature for the process variables, which is used for model accuracy. Most of the rRMSE values of all profiles range from 2.8% to 10% with very few exception. It implies that, these models can finely describe all temperature profiles of the ethanol fermentation.

Table 4.4 Accuracy of the proposed model considering (rRMSE)

Profile	rRMSE (%)		
	25 °C	30 °C	35 °C
Temperature	25 °C	30 °C	35 °C
Cell (X)	4.9665	6.7714	4.5725
Sugar (S)	4.4063	5.0231	2.8238
Ethanol (P)	10.6951	7.5309	20.8075

This result has been predicted with the consideration of the cell death rate and Leudeking-piret equation. Therefore, it could be concluded that Model II has a very significant influence on the mathematical study of the ethanol production from OPT sap through fermentation process.

4.4 Effect of initial cell concentration

For all the results presented in this section, the initial concentration of sugar was fixed to 69 g/L. The sensitivity of the model to ethanol concentration is considered. To understand the effect of cell concentration on the fermentation behaviour, we investigated the simulated conversion rate with respect to time. Figure 4.8 shows the concentration of ethanol for ratios of cell: sugar of 1:69, 2:69, and 3:69. The conversion trend of sugar to ethanol was almost similar for temperature 25°C, 30°C, and 35°C. The ethanol production was increased with the increase of cell concentration.

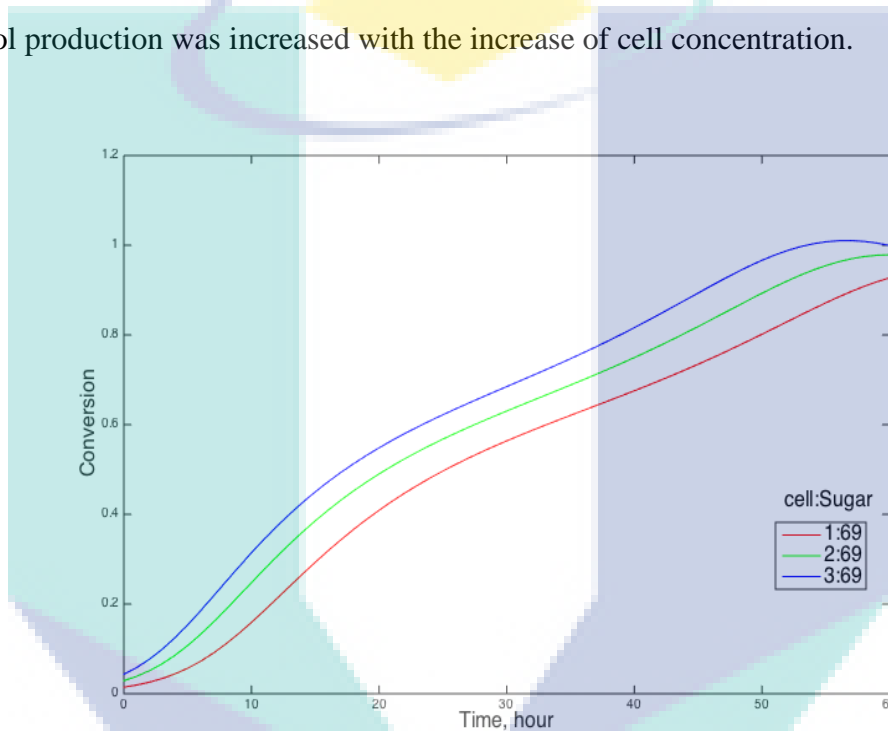


Figure 4.8 Sugar to ethanol conversion at different initial cell concentration: 1, 2 and 3g/L.

Figures 4.9-4.11 show concentration of ethanol for ratios of cell: sugar of 10:69, 15:69, and 20:69 at different temperatures. At 25°C the conversion of sugar to ethanol is increasing rapidly at early times before 30 hours, but at longer times (after 30 hours), the ethanol concentration is depleted. Even at 35°C ethanol conversion is depleted before 30 hours for high ratios 20:69 compare to other ratios. But for 30°C the conversion trend of sugar to ethanol is increased up to 40 hours. That means cell viability is longer and low inhibition is present at 30°C. In the following discussion, for ratios of cell: sugar of 10:69, 15:69, and 20:69 will be referred to as the high cell concentration case, and 1:69, 2:69, and 3:69 as the low cell concentration case.

Two distinct patterns of conversion can be identified. For low cell concentration, the conversion rate is almost constant. In contrast, for high cell concentration, the conversion grows at a constant rate up to 30 hour as indicated in Figure 4.9-4.11. Then, the conversion rate is depleted. In comparison to Figure 4.8, at initial stage, the conversion rate from sugar to ethanol for high cell concentration is higher than low cell concentration. Also, the conversion initiates earlier at higher cell concentration. It was happened due the higher initial cell concentration that can increase the rate of sugar utilization and ethanol formation (Matsushika and Sawayama 2010). Though the ethanol production rate is faster for high initial cell concentration, the cell growth is inhibited by ethanol and the conversion rate drop after short duration (within 30-60 hour). The cell inhibition slows the conversion rate by accessing the amount of ethanol. Thus, the rate of sugar consumption and ethanol production throughout fermentation depend on the concentration of cells present in the inoculum.

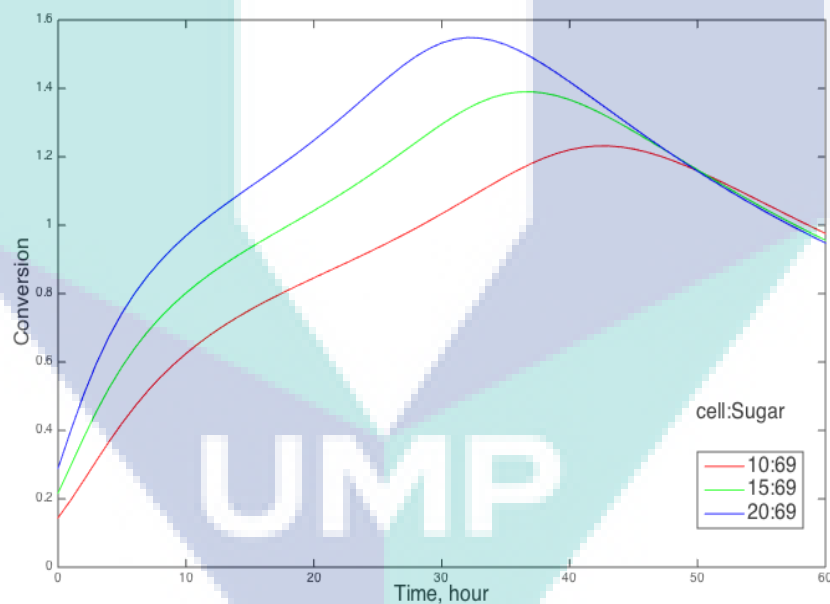


Figure 4.9 Sugar to ethanol conversion for 25°C at different initial cell concentration: 10, 15 and 20g/L.

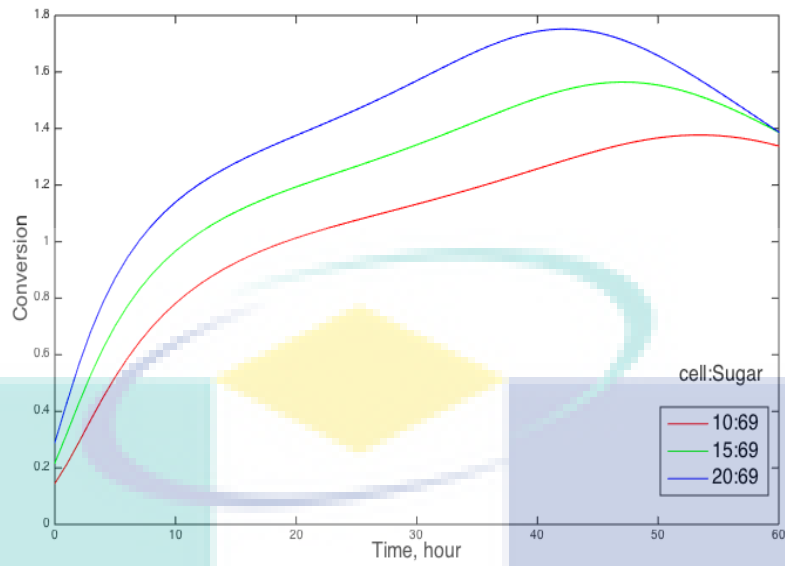


Figure 4.10 Sugar to ethanol conversion for 30°C at different initial cell

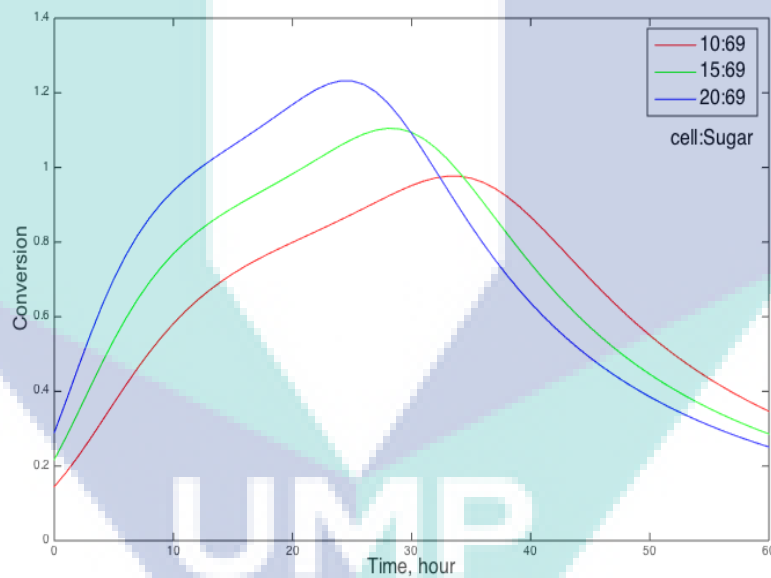
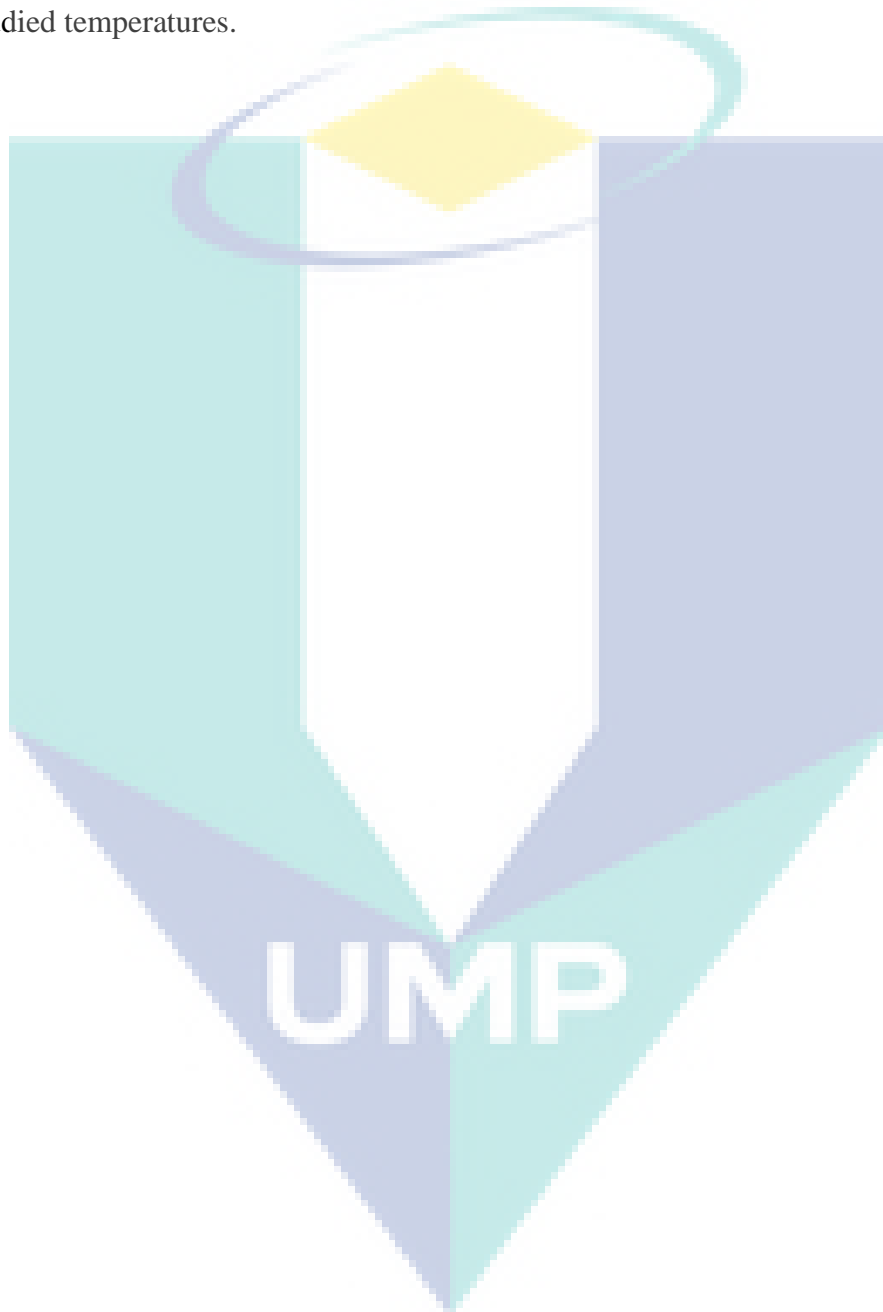


Figure 4.11 Sugar to ethanol conversion for 35°C at different initial cell concentration: 10, 15 and 20g/L.

4.5 Summary

As the fermentation process of OPT sap is a very complicated and depends on many factors, it is very difficult to establish a linear relationship between all the parameters. In this chapter, we have explained the simulation result based on modified Model I and Model II including cell death rate term, temperature dependence and Luedeking-Piret relation in substrate consumption and ethanol production. Though it is

difficult to identify the actual picture of the transformation of the fermentation process, proposed models fitted well with the experimental data. Hence, cell death rate is an influential factor in the mathematical model and should be included in formulating a fermentation process to improve the understanding of the dynamic behaviour. In summary, the mathematical models are sufficiently reliable for the experimental data for all studied temperatures.



CHAPTER 5

CONCLUSION

5.1 Introduction

This study produced new knowledge in the kinetic modelling of ethanol production from lignocellulosic biomass. Though it is difficult to understand the step by step transformation of the actual phenomenon of the fermentation, a valid mathematical model was modified of ethanol production. Our modified Model I is an extended form of Oliveira et al. (2016) and Model II is a combination of Phisalaphong et al. (2006) and Luedeking and Piret (2000) and Model I that provides a satisfactory estimate of cell growth and ethanol production using a numerical solution and nonlinear regression function. Better parameter precision was obtained by applying this approach. A Runge-Kutta algorithm was applied in Matlab and a Nelder-Mead simplex method as the optimization routine for our unknown parameter estimation. The models predicted the effects of the various temperatures on the cell activities. This approach can cover growth kinetics with cell maintenance, cell death and initial cell concentrations. In this research, the incorporation of the most important factors (substrate limitation, substrate inhibition, ethanol inhibition and cell death) for cell growth and ethanol production reflected approximately the real situation in the fermentation process.

5.2 Conclusion

To increase the accuracy of the model, the parameter estimation function should depend on the substrate limitation, substrate inhibition, ethanol inhibition and cell death simultaneously. An acceptable agreement was obtained from our proposed model with the experimental data when considered the cell death rate. The extended model improved the predictive capabilities of the dynamic behaviour to increased our

understanding on fermentation process. The influence of temperature on fermentation kinetic behaviour was also explicitly demonstrated. The models were able

to reproduce satisfactorily the behaviour of the main variables of the fermentation process of OPT sap.

An acceptable agreement was obtained from our proposed models with the experimental data. The results of the Model I and II consistently interpreted that the predicted models gave a satisfactory fit to the experimental data for all temperature of all the three bioprocess variables during the fermentation process. From the overall result discussion and parameter analysis it can be suggested that ethanol production is highly affected by temperature and the most suitable temperature is 30°C. Temperature dependency of cell growth also presented by Arrhenius relationship. The activation energy (E) for cell growth was -82.56 KJ/mol and the environment was barrier less of the system. Considering the effect of the most important factors simultaneously (substrate limitation, substrate inhibition, ethanol inhibition and cell death) increase the accuracy of the model. Therefore, the rRMSE values of all profiles was less than 15%, which indicates model I and II can finely describe all temperature profiles. The significant effect of the initial cell concentration on cell growth and ethanol production was clearly observed for the different ratios of cell concentration. Cell death rate plays a significant role in the mathematical models and should be included in formulating a fermentation process, which can serve as guidance to further optimize the ethanol fermentation process.

5.3 Recommendations for Future Research

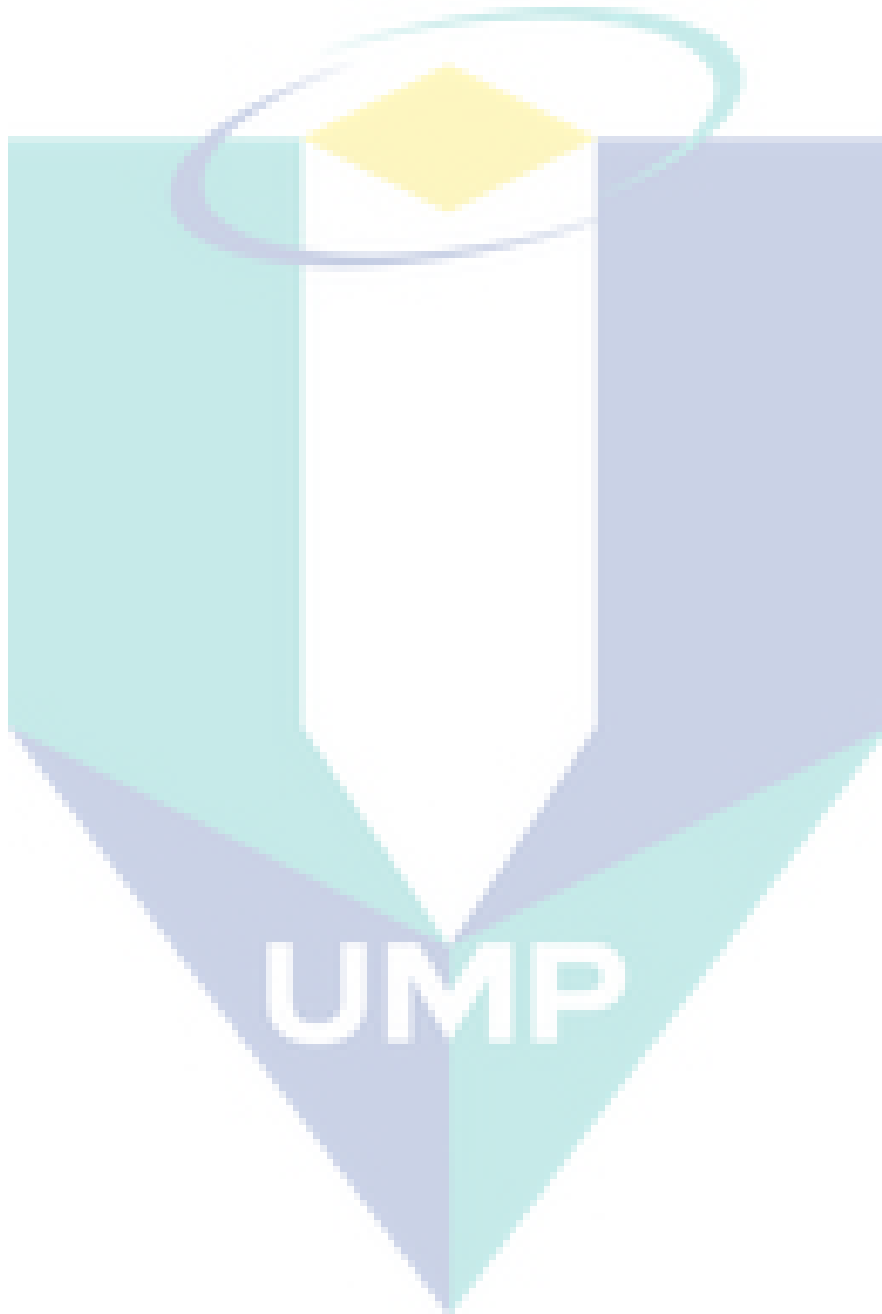
In view of present research work, the recommendations for future study may be made as follows:

i) Effect of different initial sugar concentration could be studied to reduce the inhibition of substrate concentration. Due to the time constrain the effect of pH, effect of initial nitrogen are not studied in this work.

ii) The unstructured kinetics model is the very common approach in fermentation process. To observe the ethanol inhibition at high product concentration, structured kinetics model may give better understanding.

iii) Most of the kinetic models are studied for the batch processes, therefore, models should be developed for the continues process of fermentation to produce bioethanol industrially.

iv) In this study, we used Relative Root Mean Squared Error (rRMSE) analysis for model accuracy. In future study, sensitivity analysis could be included to evaluate the impact of selected parameters.



REFERENCES

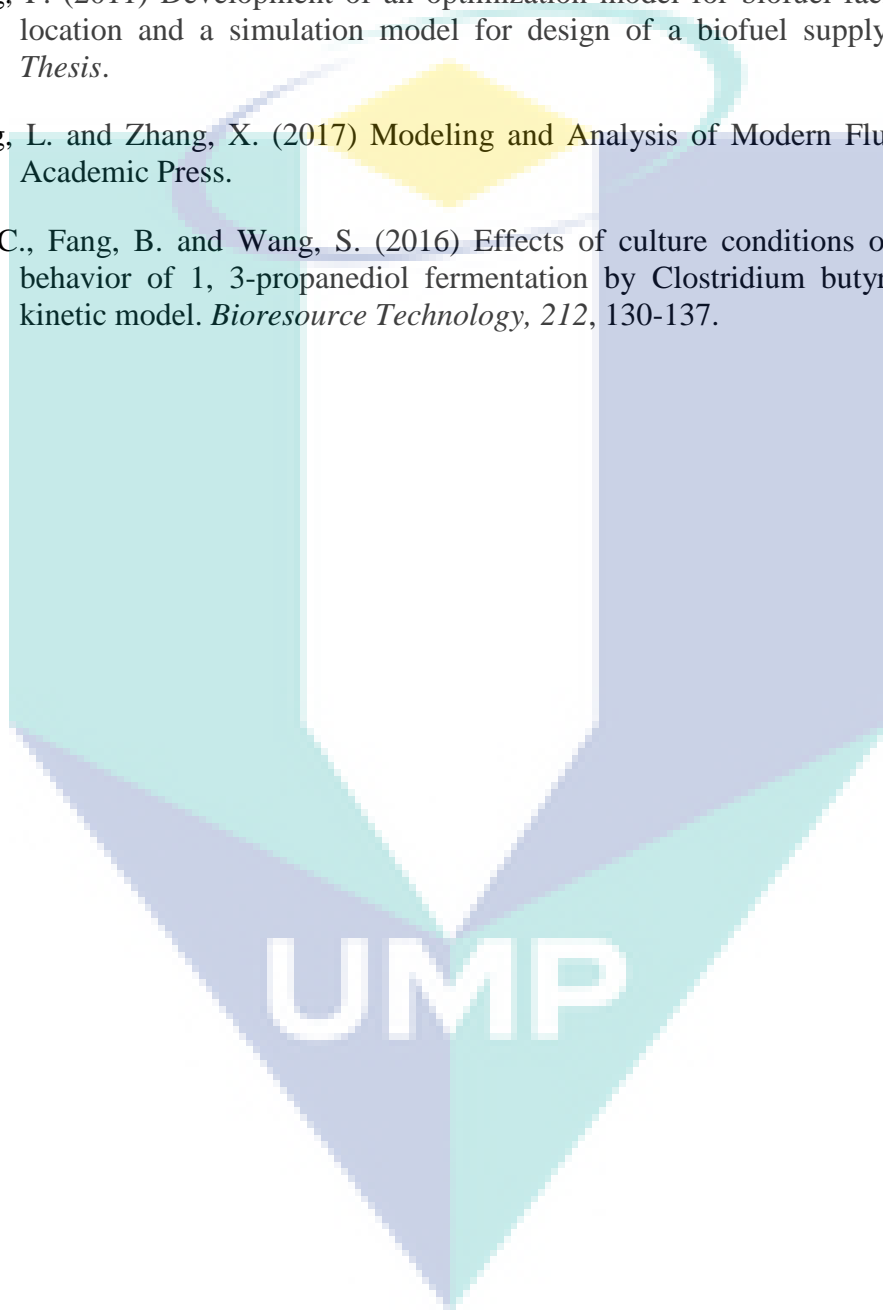
- Aiba, S. and Shoda, M. (1969) Reassessment of product inhibition in alcohol fermentation. *Journal of Fermentation Technology*, 47(12), 790.
- Alauddin, Z.A.B.Z., Lahijani, P., Mohammadi, M. and Mohamed, A.R. (2010) Gasification of lignocellulosic biomass in fluidized beds for renewable energy development: A review. *Renewable and Sustainable Energy Reviews*, 14(9), 2852-2862.
- Badger, P. (2002) Ethanol from cellulose: a general review. *Trends in new crops and new uses*, 1, 17-21.
- Bansal, P., Hall, M., Realff, M.J., Lee, J.H. and Bommarius, A.S. (2009) Modeling cellulase kinetics on lignocellulosic substrates. *Biotechnology advances*, 27(6), 833-848.
- Beale, C.M., Lennon, J.J., Yearsley, J.M., Brewer, M.J. and Elston, D.A. (2010) Regression analysis of spatial data. *Ecology Letters*, 13(2), 246-264.
- Biröl, G., Doruker, P., Kirdar, B., Önsan, Z.İ. and Ülgen, K. (1998) Mathematical description of ethanol fermentation by immobilised *Saccharomyces cerevisiae*. *Process Biochemistry*, 33(7), 763-771.
- Bosse, T. and Griewank, A. (2014) Optimal control of beer fermentation processes with Lipschitz-constraint on the control. *Journal of the Institute of Brewing*, 120(4), 444-458.
- Clark, D.S. and Blanch, H.W. (1996) *Biochemical Engineering*, Marcel Dekker, Inc, USA.
- Costa, R.S., Hartmann, A. and Vinga, S. (2016) Kinetic modeling of cell metabolism for microbial production. *Journal of Biotechnology*, 219, 126-141.
- Esfahanian, M., Rad, A.S., Khoshhal, S., Najafpour, G. and Asghari, B. (2016) Mathematical modeling of continuous ethanol fermentation in a membrane bioreactor by pervaporation compared to conventional system: Genetic algorithm. *Bioresource Technology*, 212, 62-71.
- Fan, S., Chen, S., Tang, X., Xiao, Z., Deng, Q., Yao, P., Sun, Z., Zhang, Y. and Chen, C. (2015) Kinetic model of continuous ethanol fermentation in closed-circulating process with pervaporation membrane bioreactor by *Saccharomyces cerevisiae*. *Bioresource Technology*, 177, 169-175.
- Garnier, A. and Gaillet, B. (2015) Analytical solution of Luedeking–Piret equation for a batch fermentation obeying Monod growth kinetics. *Biotechnology and Bioengineering*, 112(12), 2468-2474.
- Ghaly, A. and El-Taweel, A. (1994) Kinetics of batch production of ethanol from cheese whey. *Biomass and Bioenergy*, 6(6), 465-478.

- Ghose, T. and Tyagi, R. (1979) Rapid ethanol fermentation of cellulose hydrolysate. II. Product and substrate inhibition and optimization of fermentor design. *Biotechnology and Bioengineering*, 21(8), 1401-1420.
- Griggs, A.J., Stickel, J.J. and Lischeske, J.J. (2012a) A mechanistic model for enzymatic saccharification of cellulose using continuous distribution kinetics I: depolymerization by EGI and CBHI. *Biotechnology and Bioengineering*, 109(3), 665-675.
- Griggs, A.J., Stickel, J.J. and Lischeske, J.J. (2012b) A mechanistic model for enzymatic saccharification of cellulose using continuous distribution kinetics II: cooperative enzyme action, solution kinetics, and product inhibition. *Biotechnology and Bioengineering*, 109(3), 676-685.
- Guidini, C.Z., Marquez, L.D.S., de Almeida Silva, H., de Resende, M.M., Cardoso, V.L. and Ribeiro, E.J. (2014) Alcoholic fermentation with flocculant *Saccharomyces cerevisiae* in fed-batch process. *Applied Biochemistry and Biotechnology*, 172(3), 1623-1638.
- Halim, N.B.A. (2016) Optimization of bioethanol production from oil palm trunk sap, Universiti Malaysia Pahang.
- Himmel, M.E., Ding, S.-Y., Johnson, D.K., Adney, W.S., Nimlos, M.R., Brady, J.W. and Foust, T.D. (2007) Biomass recalcitrance: engineering plants and enzymes for biofuels production. *Science*, 315(5813), 804-807.
- Hinshelwood, C.N. (1946) The chemical kinetics of the bacterial cell, Oxford: The Clarendon Press, UK.
- Hoppe, G.K. and Hansford, G.S. (1982) Ethanol inhibition of continuous anaerobic yeast growth. *Biotechnology Letters*, 4(1), 39-44.
- Hossain, N. and Jalil, R. (2015) Sugar and bioethanol production from oil palm trunk (OPT). *Asia Pacific Journal of Energy and Environment*, 2(2), 81-84.
- Jamil, N.M. and Wang, Q. (2016) The Nondimensionalization of Equations Describing Enzymatic Cellulose Hydrolysis. *World Applied Sciences Journal*, 34(2), 158-163.
- Jin, H., Liu, R. and He, Y. (2012) Kinetics of batch fermentations for ethanol production with immobilized *Saccharomyces cerevisiae* growing on sweet sorghum stalk juice. *Procedia Environmental Sciences*, 12, 137-145.
- Kelkar, S. and Dolan, K. (2012) Modeling the effects of initial nitrogen content and temperature on fermentation kinetics of hard cider. *Journal of Food Engineering*, 109(3), 588-596.
- Khalifa, N. (2011) Empirical and kinetic models for the determination of pharmaceutical product stability.

- Limayem, A. and Ricke, S.C. (2012) Lignocellulosic biomass for bioethanol production: current perspectives, potential issues and future prospects. *Progress in Energy and Combustion Science*, 38(4), 449-467.
- Liu, J.-Z., Weng, L.-P., Zhang, Q.-L., Xu, H. and Ji, L.-N. (2003) A mathematical model for gluconic acid fermentation by *Aspergillus niger*. *Biochemical engineering journal*, 14(2), 137-141.
- Liu, Z. and Li, X. (2014) The kinetics of ethanol fermentation based on adsorption processes. *Kemija u Industriji*, 63(7-8).
- Luedeking, R. and Piret, E.L. (2000) A kinetic study of the lactic acid fermentation. Batch process at controlled pH. *Biotechnology and Bioengineering*, 67(6), 636-644.
- Matsuoka, Y. and Shimizu, K. (2015) Current status and future perspectives of kinetic modeling for the cell metabolism with incorporation of the metabolic regulation mechanism. *Bioresources and Bioprocessing*, 2(1), 1-19.
- Matsushika, A. and Sawayama, S. (2010) Effect of initial cell concentration on ethanol production by flocculent *Saccharomyces cerevisiae* with xylose-fermenting ability. *Applied Biochemistry and Biotechnology*, 162(7), 1952-1960.
- Mohamad, N.L., Kamal, S.M.M., Mokhtar, M.N., Husain, S.A. and Abdullah, N. (2016) Dynamic mathematical modelling of reaction kinetics for xylitol fermentation using *Candida tropicalis*. *Biochemical engineering journal*, 111, 10-17.
- Monod, J. (1949a) The growth of bacterial cultures. *A. Rev. Microbiol*, 3, 371-394.
- Monod, J. (1949b) The growth of bacterial cultures. *Annual Reviews in Microbiology*, 3(1), 371-394.
- Oliveira, S.C., Oliveira, R.C., Tacin, M.V. and Gattás, E.A. (2016) Kinetic modeling and optimization of a batch ethanol fermentation process. *Journal of Bioprocessing & Biotechniques*, 6, 266.
- Ona, I., Agogo, H. and Iorungwa, M. (2019) Production of Bioethanol from Cassava using *Zymomonas mobilis*: Effect of Temperature and Substrate concentration. *NIGERIAN ANNALS OF PURE AND APPLIED SCIENCES*, 1(1), 153-160.
- Papagianni, M., Boonpooh, Y., Matthey, M. and Kristiansen, B. (2007) Substrate inhibition kinetics of *Saccharomyces cerevisiae* in fed-batch cultures operated at constant glucose and maltose concentration levels. *Journal of industrial microbiology & biotechnology*, 34(4), 301-309.
- Phisalaphong, M., Srirattana, N. and Tanthapanichakoon, W. (2006) Mathematical modeling to investigate temperature effect on kinetic parameters of ethanol fermentation. *Biochemical engineering journal*, 28(1), 36-43.
- Rivera, E.C., Da Costa, A.C., Lunelli, B.H., Maciel, M.R.W. and Maciel Filho, R. (2008) Kinetic modeling and parameter estimation in a tower bioreactor for

- bioethanol production. *Applied biochemistry and biotechnology*, 148(1-3), 163-173.
- Rivera, E.C., Yamakawa, C.K., Saad, M.B., Atala, D.I., Ambrosio, W.B., Bonomi, A., Junior, J.N. and Rossell, C.E. (2016) Effect of temperature on sugarcane ethanol fermentation: Kinetic modeling and validation under very-high-gravity fermentation conditions. *Biochemical engineering journal*.
- Salgado, J.M., Converti, A. and Domínguez, J.M. (2012) D-Xylitol, pp. 161-191, Springer.
- Sampaio, F.C., Mantovani, H.C., Passos, F.J.V., de Moraes, C.A., Converti, A. and Passos, F.M.L. (2005) Bioconversion of d-xylose to xylitol by *Debaryomyces hansenii* UFV-170: Product formation versus growth. *Process Biochemistry*, 40(11), 3600-3606.
- Samsudin, M.D.M. and Don, M.M. (2015) Assessment of bioethanol yield by *S. cerevisiae* grown on oil palm residues: Monte Carlo simulation and sensitivity analysis. *Bioresource Technology*, 175, 417-423.
- Silva, C.J., Mussatto, S.I. and Roberto, I.C. (2006) Study of xylitol production by *Candida guilliermondii* on a bench bioreactor. *Journal of Food Engineering*, 75(1), 115-119.
- Silva, S.S., Roberto, I.C., Felipe, M.G. and Mancilha, I.M. (1996) Batch fermentation of xylose for xylitol production in stirred tank bioreactor. *Process Biochemistry*, 31(6), 549-553.
- Srimachai, T., Nuithitikul, K., Sompong, O., Kongjan, P. and Panpong, K. (2015) Optimization and kinetic modeling of ethanol production from oil palm frond juice in batch fermentation. *Energy Procedia*, 79, 111-118.
- Talib, A.T., Mokhtar, M.N., Baharuddin, A.S. and Sulaiman, A. (2014) Effects of aeration rate on degradation process of oil palm empty fruit bunch with kinetic-dynamic modeling. *Bioresource Technology*, 169, 428-438.
- Tian, Y.-C., Zhang, T., Yao, H. and Tadé, M.O. (2014) Computation of mathematical models for complex industrial processes, World Scientific.
- Vázquez, J.A. and Murado, M.A. (2008) Unstructured mathematical model for biomass, lactic acid and bacteriocin production by lactic acid bacteria in batch fermentation. *Journal of Chemical Technology and Biotechnology*, 83(1), 91-96.
- Wang, F.-S. and Sheu, J.-W. (2000) Multiobjective parameter estimation problems of fermentation processes using a high ethanol tolerance yeast. *Chemical Engineering Science*, 55(18), 3685-3695.
- Wang, L., Agyemang, S.A., Amini, H. and Shahbazi, A. (2015) Mathematical modeling of production and biorefinery of energy crops. *Renewable and Sustainable Energy Reviews*, 43, 530-544.

- Wang, Y. and Liu, S. (2014) Kinetic modeling of ethanol batch fermentation by *Escherichia coli* FBWHR using hot-water sugar maple wood extract hydrolyzate as substrate. *Energies*, 7(12), 8411-8426.
- You, L. and Baharin, B. (2006) Effects of enzymatic hydrolysis on crude palm olein by lipase from *Candida rugosa*. *Journal of Food Lipids*, 13(1), 73-87.
- Zhang, F. (2011) Development of an optimization model for biofuel facility size and location and a simulation model for design of a biofuel supply chain. *PhD Thesis*.
- Zheng, L. and Zhang, X. (2017) *Modeling and Analysis of Modern Fluid Problems*, Academic Press.
- Zhu, C., Fang, B. and Wang, S. (2016) Effects of culture conditions on the kinetic behavior of 1, 3-propanediol fermentation by *Clostridium butyricum* with a kinetic model. *Bioresource Technology*, 212, 130-137.



APPENDIX A

Model I coding at 25°C temperature

Parameter estimation

```
function S = Sfun2D1(b)
% computation of an error function for an ODE model
% INPUT: b - vector of parameters

global tdata xdata x0

%% ODE model
% (nested function, uses parameters b(1) to b(6) of the main function)
function dx = f(t,x)
    dx = zeros(3,1);
    pmax=29.9024;
    n=1.753;

    dx(1)=b(1)*x(3)/(b(2)+x(3)+(x(3)^2/b(3)))*((1-x(2)/pmax)^n)*x(1)-b(6)*x(1);
    dx(2)=b(5)*b(1)*x(3)/(b(2)+x(3)+(x(3)^2/b(3)))*(1-x(2)/pmax)^n*x(1);
    dx(3)=-b(5)*b(1)*x(3)/((b(2)+x(3)+(x(3)^2/b(3)))*b(4))*(1-x(2)/pmax)^n*x(1);

end

%% numerical integration set up

tspan = [0:1:max(tdata)];
[tsol,xsol] = ode15s(@f,tspan,x0);

%% plot result of the integration

figure(1)
for i = 1:3
    subplot(1,3,i)
    plot(tdata,xdata(:,i),'x','MarkerSize',10);
    hold on
    plot(tsol,xsol(:,i));
    hold off
    ylabel(['x(' num2str(i) ')']);
end
%drawnow

%% find predicted values x(tdata)

xpred = interp1(tsol,xsol,tdata);
```



```
%% compute total error
```

```
S = 0;
```

```
for i = 1:length(tdata)
```

```
    S = S + sum((xpred(i,:)-xdata(i,:)).^2);
```

```
end
```

```
end
```

```
function paramfit2D
```

```
% main program for fitting parameters of an ODE model to data
```

```
% the model and the error function are defined in the file Sfun2D.m
```

```
%clearvars -global
```

```
global tdata xdata x0
```

```
%% data for the model
```

```
% time - value of 1st variable - value of 2nd variable - value of 3rd
```

```
% variable
```

```
tdata=(1:50);
```

```
xdata=zeros(50,3);
```

```
xdata(:,1)=[1.25;2.20;3.45;4.76;6.07;7.37;8.74;9.01;11.12;12.43;13.74;15.05;16.30;17.  
55;18.45;19.59;20.73;21.81;22.77;23.63;24.48;25.22;25.84;26.35;26.81;27.15;27.43;28  
.60;28.72;29.72;29.72;30.60;31.47;32.32;32.15;32.86;32.64;32.47;32.18;32.90;33.61;3  
3.39;33.50;33.65;33.82;33.76;33.76;33.76;33.76;33.82];;
```

```
xdata(:,2)=[2.74;3.76;4.73;5.75;6.71;7.74;8.82;9.61;10.63;11.66;12.68;13.70;14.67;15.  
64;16.43;17.28;18.31;19.10;19.95;20.75;21.54;22.23;22.68;23.36;23.93;24.44;24.95;25  
.41;25.81;26.09;26.43;26.77;27.11;27.34;27.57;27.8;28.02;28.14;28.36;28.53;28.70;28.  
82;28.93;29.10;29.22;29.39;29.50;29.61;29.73;29.90];
```

```
xdata(:,3)=[86.63;82.92;82.48;82.11;81.85;81.4;80.95;80.5;80;78.78;77.97;76.44;75.07  
;72.84;71.03;68.96;67.16;66.5;61.29;58.95;57.25;57;54.45;53.46;51.97;51.3;50.98;50.4  
;50.13;50;49.5;49.32;49.14;49.14;48;48.69;48.69;48.58;48.6;48.7;48.32;48.33;48;48.05  
;47.96;47.88;47.97;47.7;47;46.67];
```

```
%% initial conditions
```

```
x0(1) = 1.25;
```

```
x0(2) = 2.74;
```

```
x0(3) = 86.63;
```

```
%% initial guess of parameter values 25 deg temp
```

```
b(1)=0.9921;
```

```
b(2)=0.0162;  
b(3)=40.1792;  
b(4)=0.6506;  
b(5)=0.7598;  
b(6)=0.0021;
```

```
%% minimization step
```

```
[bmin, Smin] = fminsearch(@Sfun2D1,b);
```

```
disp('Estimated parameters b(i):');  
disp(bmin)  
disp('Smallest value of the error S:');  
disp(Smin)
```

```
end
```

Main coding

```
function rk4_fermentation (a, b, N, alpha)
```

```
alpha= [1.25 2.74 86.63]; %initial value for y1, y2, and y3  
b=50;  
a=0;  
N=50;
```

```
m = size(alpha,1);  
if m == 1  
    alpha = alpha';  
end
```

```
h = (b-a)/N; %the step size  
t (1) = a;  
w(:,1) = alpha; %initial conditions
```

```
for i = 1:N  
    k1 = h*f(t(i), w(:,i));  
    k2 = h*f(t(i)+h/2, w(:,i)+0.5*k1);  
    k3 = h*f(t(i)+h/2, w(:,i)+0.5*k2);  
    k4 = h*f(t(i)+h, w(:,i)+k3);  
    w(:,i+1) = w(:,i) + (k1 + 2*k2 + 2*k3 + k4)/6;  
    t(i+1) = a + i*h;  
end
```


%w(1,:), w(2,:), w(3,:) listing for y(1), y(2), and y(3) respectively

[t' w']; % transpose matrix

ts= (1:50);

tnew= [1 5 10 15 20 25 30 35 40 45 50];

%experimental results at temperature = 25 degree Celsius

cell=[1.25;2.20;3.45;4.76;6.07;7.37;8.74;9.01;11.12;12.43;13.74;15.05;16.30;17.55;18.45;19.59;20.73;21.81;22.77;23.63;24.48;25.22;25.84;26.35;26.81;27.15;27.43;28.60;28.72;29.72;29.72;30.60;31.47;32.32;32.15;32.86;32.64;32.47;32.18;32.90;33.61;33.39;33.50;33.65;33.82;33.76;33.76;33.76;33.76;33.82];

cellnew=[1.25;6.07;12.43;18.45;23.63;26.81;29.72;32.15;32.90;33.82;33.82];

ethanol=[2.74;3.76;4.73;5.75;6.71;7.74;8.82;9.61;10.63;11.66;12.68;13.70;14.67;15.64;16.43;17.28;18.31;19.10;19.95;20.75;21.54;22.23;22.68;23.36;23.93;24.44;24.95;25.41;25.81;26.09;26.43;26.77;27.11;27.34;27.57;27.8;28.02;28.14;28.36;28.53;28.70;28.82;28.93;29.10;29.22;29.39;29.50;29.61;29.73;29.9024];

ethanolnew=[2.74;6.71;11.66;16.43;20.75;23.93;26.09;27.57;28.53;29.22;29.90];

sugar=[86.63;82.92;82.48;82.11;81.85;81.4;80.95;80.5;80;78.78;77.97;76.44;75.07;72.84;71.03;68.96;67.16;66.5;61.29;58.95;57.25;57;54.45;53.46;51.97;51.3;50.98;50.4;50.13;50;49.5;49.32;49.14;49.14;48;48.69;48.69;48.58;48.6;48.7;48.32;48.33;48;48.05;47.96;47.88;47.97;47.7;47;46.67];

sugarnew=[86.63;81.85;78.78;71.03;58.95;51.97;50;48;48.7;47.96;46.67];

plot (t, w (1, :),'g',t, w(2,:),'r',t, w(3,:),'b')

hold on

plot (tnew, cellnew, 'o',tnew, ethanolnew, '^',tnew, sugarnew, 'square', 'MarkerFaceColor',[.1 .5 .1])

legend ('predicted cell','predicted ethanol','predicted sugar','data cell','data ethanol','data sugar')

%Relative root mean squared error (rRMSE) for model accuracy

N=50;

meanCell = sum(cell)/N;

meanEthanol = sum(ethanol)/N;

meanSugar = sum(sugar)/N;

w1=w(1,1:50)';

w2=w(2,1:50)';

w3=w(3,1:50)';

```

rmseCell=100*(1/meanCell)*sqrt(1/N*sum((w1-cell).^2))
rmseEthanol=100*(1/meanEthanol)*sqrt(1/N*sum((w2-ethanol).^2))
rmseSugar=100*(1/meanSugar)*sqrt(1/N*sum((w3-sugar).^2))

```

```
function dy = f(t, y)
```

```
% estimated values
```

```

mum=1.1680;
ks=0.0397;
ki=26.1107;
kd=0.0001;
yps=0.6520;
alpha=0.7872;
pmax=29.9024;
n=1.753;

```

```

dy=[(mum*y(3)/(ks+y(3)+(y(3)^2/ki))*(1-y(2)/pmax)^n)*y(1)-kd*y(1);
(alpha*mum*y(3)/(ks+y(3)+(y(3)^2/ki))*(1-y(2)/pmax)^n)*y(1);
-(alpha*mum*y(3)/((ks+y(3)+(y(3)^2/ki))*yps)*(1-y(2)/pmax)^n)*y(1)];

```

Model I coding at 30°C temperature

Parameter estimation

```
function S = Sfun2D1(b)
```

```

% computation of an error function for an ODE model
% INPUT: b - vector of parameters

```

```
global tdata xdata x0
```

```
%% ODE model
```

```
% (nested function, uses parameters b(1) and b(2) of the main function)
```

```
function dx = f(t,x)
```

```

dx = zeros(3,1);
pmax=30.76;
n=1.753;

```

```

dx(1)=b(1)*x(3)/(b(2)+x(3)+(x(3)^2/b(3)))*((1-x(2)/pmax)^n)*x(1)-b(6)*x(1);
dx(2)=b(5)*b(1)*x(3)/(b(2)+x(3)+(x(3)^2/b(3)))*(1-x(2)/pmax)^n*x(1);
dx(3)=-b(5)*b(1)*x(3)/((b(2)+x(3)+(x(3)^2/b(3)))*b(4))*(1-x(2)/pmax)^n*x(1);

```

```
end
```

```

%% numerical integration set up

tspan = [0:1:max(tdata)];
[tsol,xsol] = ode15s(@f,tspan,x0);

%% plot result of the integration

figure(1)
for i = 1:3
    subplot(1,3,i)
    plot(tdata,xdata(:,i),'x','MarkerSize',10);
    hold on
    plot(tsol,xsol(:,i));
    hold off
    ylabel(['x(' num2str(i) ')']);
end

%% find predicted values x(tdata)

xpred = interp1(tsol,xsol,tdata);

%% compute total error

S = 0;
for i = 1:length(tdata)
    S = S + sum((xpred(i,:)-xdata(i,:)).^2);
end
end

-----

function paramfit2D

% main program for fitting parameters of an ODE model to data
% the model and the error function are defined in the file Sfun2D.m

%clearvars -global
global tdata xdata x0

tdata=(1:50);
xdata=zeros(50,3);
xdata
(:,1)=[1.25;5.66;7.16;8.54;10.14;11.81;13.41;15.08;16.47;18.13;19.74;21.36;22.67;24.2
8;25.74;27.15;28.36;29.63;30.89;32.69;33.02;34;35.32;35.56;36.18;36.76;37.15;37.67;

```

```
37.73;37.9;38.02;38.13;38.13;38.02;37.95;37.79;37.6;37.5;37.33;37.04;36.87;36.64;36.64;36.24;36.06;35.95;35.76;35.8;35.66;35.6];
```

```
xdata
```

```
(:,2)=[4.30;5.28;6.31;7.12;8.15;9.24;10.28;11.31;12.23;13.21;14.24;15.11;16.20;17.23;18.15;19.07;19.88;20.68;21.54;22.29;22.92;23.61;24.19;24.73;25.16;25.62;26.03;26.37;26.54;26.83;27.06;27.23;27.35;27.46;27.52;27.63;27.63;27.63;27.69;28.69;28.69;28.81;29.38;29.84;30.19;30.76;29.30;29.01;28.61;28.38];
```

```
xdata
```

```
(:,3)=[86.63;82.03;79.50;77.96;77.51;77.06;75.03;73.85;72.08;71.50;70.18;69.03;68.20;67.35;66.05;64.45;63.31;60.04;57.40;55.06;53.36;53.11;50.56;49.57;48.08;47.41;47.09;46.51;46.24;46.11;45.61;45.43;45.25;45.25;44.11;44.80;44.80;44.69;44.71;44.81;44.43;44.44;44.11;44.16;44.07;43.99;44.08;43.81;43.11;42.78];
```

```
%% initial conditions
```

```
x0(1) = 1.25;  
x0(2) = 4.30;  
x0(3) = 86.63;
```

```
%% initial guess of parameter values 30 deg temp
```

```
b(1)=0.5557; %mum  
b(2)=0.0991; %ks  
b(3)=220.3900; %ki  
b(4)=0.5820; %yps  
b(5)=0.6212; %alpha  
b(6)=0.0032; %kd
```

```
%% minimization step
```

```
[bmin, Smin] = fminsearch(@Sfun2D1,b);
```

```
disp('Estimated parameters b(i):');  
disp(bmin)  
disp('Smallest value of the error S:');  
disp(Smin)
```

```
end
```

Main coding

```
function rk4_fermentation (a, b, N, alpha)

alpha=[1.25 4.30 86.63]; %initial value for y1, y2, and y3
b=50;
a=0;
N=50;

m = size(alpha,1);
if m == 1
    alpha = alpha';
end

h = (b-a)/N; %the step size
t(1) = a;
w(:,1) = alpha; %initial conditions

for i = 1:N
    k1 = h*f(t(i), w(:,i));
    k2 = h*f(t(i)+h/2, w(:,i)+0.5*k1);
    k3 = h*f(t(i)+h/2, w(:,i)+0.5*k2);
    k4 = h*f(t(i)+h, w(:,i)+k3);
    w(:,i+1) = w(:,i) + (k1 + 2*k2 + 2*k3 + k4)/6;
    t(i+1) = a + i*h;
end

[t' w']; %transpose matrix

ts=(1:50);

tnew=[1 5 10 15 20 25 30 35 40 45 50];

%experimental results at temperature = 30 degree celcius

cell=[1.25;5.66;7.16;8.54;10.14;11.81;13.41;15.08;16.47;18.13;19.74;21.36;22.67;24.2
8;25.74;27.15;28.36;29.63;30.89;32.69;33.02;34;35.32;35.56;36.18;36.76;37.15;37.67;
37.73;37.9;38.02;38.13;38.13;38.02;37.95;37.79;37.6;37.5;37.33;37.04;36.87;36.64;36.
64;36.24;36.06;35.95;35.76;35.8;35.66;35.6];
cellnew=[1.25;10.14;18.13;25.74;32.69;36.18;37.9;37.95;37.04;36.06;35.6];
ethanol=[4.30;5.28;6.31;7.12;8.15;9.24;10.28;11.31;12.23;13.21;14.24;15.11;16.20;17.
23;18.15;19.07;19.88;20.68;21.54;22.29;22.92;23.61;24.19;24.73;25.16;25.62;26.03;26
.37;26.54;26.83;27.06;27.23;27.35;27.46;27.52;27.63;27.63;27.63;27.69;28.69;28.69;2
8.81;29.38;29.84;30.19;30.76;29.30;29.01;28.61;28.38];
ethanolnew=[4.30;8.15;13.21;18.15;22.29;25.16;26.83;27.52;28.69;30.19;28.38];
sugar=[86.63;82.03;79.50;77.96;77.51;77.06;75.03;73.85;72.08;71.50;70.18;69.03;68.2
0;67.35;66.05;64.45;63.31;60.04;57.40;55.06;53.36;53.11;50.56;49.57;48.08;47.41;47.
```

```

09;46.51;46.24;46.11;45.61;45.43;45.25;45.25;44.11;44.80;44.80;44.69;44.71;44.81;44
.43;44.44;44.11;44.16;44.07;43.99;44.08;43.81;43.11;42.78];
sugarnew=[86.63;77.51;71.50;66.05;55.06;48.08;46.11;44.11;44.81;44.07;42.78];

```

```

plot(t, w(1,:), 'g', t, w(2,:), 'r', t, w(3,:), 'b')
hold on
plot(tnew, cellnew, 'o', tnew, ethanolnew, '^', tnew,
sugarnew, 'square', 'MarkerFaceColor', [1 .5 .1])
legend('predicted cell', 'predicted ethanol', 'predicted sugar', 'data cell', 'data ethanol', 'data
sugar')

```

```

%Relative root mean squared error (rRMSE) for model accuracy

```

```

N=50;
meanCell = sum(cell)/N;
meanEthanol = sum(ethanol)/N;
meanSugar = sum(sugar)/N;

```

```

w1=w(1,1:50);
w2=w(2,1:50);
w3=w(3,1:50);

```

```

rmseCell=100*(1/meanCell)*sqrt(1/N*sum((w1-cell).^2))
rmseEthanol=100*(1/meanEthanol)*sqrt(1/N*sum((w2-ethanol).^2))
rmseSugar=100*(1/meanSugar)*sqrt(1/N*sum((w3-sugar).^2))

```

```

function dy = f(t, y)
%estimated values
mum=0.5779;
ks=0.0277;
ki=183.4506;
kd=0.0068;
yps=0.5836;
alpha=0.5672;
pmax=30.76;
n=1.653;

```

```

dy =[(mum*y(3)/(ks+y(3)+(y(3)^2/ki))*(1-y(2)/pmax)^n)*y(1)-kd*y(1);
(alpha*mum*y(3)/(ks+y(3)+(y(3)^2/ki))*(1-y(2)/pmax)^n)*y(1);
-(alpha*mum*y(3)/((ks+y(3)+(y(3)^2/ki))*yps)*(1-y(2)/pmax)^n)*y(1)];

```

Model I coding at 35°C temperature

Parameter estimation

```
function S = Sfun2D1(b)
% computation of an error function for an ODE model
% INPUT: b - vector of parameters

global tdata xdata x0

%% ODE model
% (nested function, uses parameters b(1) and b(2) of the main function)
function dx = f(t,x)
    dx = zeros(3,1);
    pmax=26.06;
    n=2;

    dx(1)=b(1)*x(3)/(b(2)+x(3)+(x(3)^2/b(3)))*((1-x(2)/pmax)^n)*x(1)-b(6)*x(1);
    dx(2)=b(5)*b(1)*x(3)/(b(2)+x(3)+(x(3)^2/b(3)))*(1-x(2)/pmax)^n*x(1);
    dx(3)=-b(5)*b(1)*x(3)/((b(2)+x(3)+(x(3)^2/b(3)))*b(4))*(1-x(2)/pmax)^n*x(1);
end

%% numerical integration set up

tspan = [0:1:max(tdata)];
[tsol,xsol] = ode15s(@f,tspan,x0);

%% plot result of the integration

figure(1)
for i = 1:3
    subplot(1,3,i)
    plot(tdata,xdata(:,i),'x','MarkerSize',10);
    hold on
    plot(tsol,xsol(:,i));
    hold off
    ylabel(['x(' num2str(i) ')']);
end

%% find predicted values x(tdata)

xpred = interp1(tsol,xsol,tdata);

%% compute total error

S = 0;
for i = 1:length(tdata)
    S = S + sum((xdata(i,:)-xpred(i,:)).^2);
end
```

end

```
function paramfit2D
```

```
% main program for fitting parameters of an ODE model to data  
% the model and the error function are defined in the file Sfun2D.m
```

```
%clearvars -global  
global tdata xdata x0
```

```
tdata=(1:50);  
xdata=zeros(50,3);  
xdata(:,1)=[1.25;2.71;2.89;3.35;3.65;4.14;4.44;4.70;5.27;5.58;7.11;8.33;10.83;11.91;12  
.57;13.63;14.89;15.88;16.94;17.77;19.59;20.42;21.05;21.59;22.93;24.39;25.66;26.90;2  
6.75;27.98;28.05;28.14;29.14;30.14;30.45;30.86;30.98;31.20;31.74;31.86;32.51;32.77;  
33.19;33.41;33.24;33.11;33.00;32.95;32.50;32.50];  
xdata(:,2)=[1.011;1.121;2.021;2.041;2.051;3.061;3.071;3.073;4.079;4.081;4.13;5.74;5.8  
8;7.08;8.79;9.97;10.09;12.08;14.40;16.00;17.35;18.42;21.08;20.21;20.83;21.37;21.80;2  
2.29;22.67;22.96;23.25;23.59;23.83;24.03;24.27;24.59;24.70;24.95;24.95;25.04;25.24;  
25.33;25.43;25.52;25.62;25.82;25.87;25.92;26.01;26.06];  
xdata(:,3)=[86.63;86.26;85.82;85.45;85.19;84.74;84.29;83.84;82.93;82.12;81.31;79.78;  
78.41;76.18;74.37;72.30;70.50;68.43;64.63;62.29;60.59;58.97;57.79;56.80;55.31;54.64  
;54.32;53.74;53.47;53.02;52.84;52.66;52.48;52.48;52.39;52.03;52.03;51.92;51.94;51.8  
9;51.66;51.67;51.48;51.39;51.30;51.22;51.31;51.04;50.79;50.01];
```

```
%% initial conditions
```

```
x0(1) = 1.25;  
x0(2) = 1.011;  
x0(3) = 86.63;
```

```
%% initial guess of parameter values 35 deg temp
```

```
b(1)=0.4750;  
b(2)=0.0520;  
b(3)=180.31;  
b(4)=0.7101;  
b(5)=0.7501;  
b(6)=0.0041;  
%b(6)=kd
```

```
%% minimization step
```



```
[bmin, Smin] = fminsearch(@Sfun2D1,b);
```

```
disp('Estimated parameters b(i):');  
disp(bmin)  
disp('Smallest value of the error S:');  
disp(Smin)
```

```
end
```

Main coding

```
function rk4_fermentation (a, b, N, alpha)
```

```
alpha=[1.25 1.011 86.63]; %initial value for y1, y2, and y3  
b=50;  
a=0;  
N=50;
```

```
m = size(alpha,1);  
if m == 1  
    alpha = alpha';  
end
```

```
h = (b-a)/N; %the step size  
t(1) = a;  
w(:,1) = alpha; %initial conditions
```

```
for i = 1:N  
    k1 = h*f(t(i), w(:,i));  
    k2 = h*f(t(i)+h/2, w(:,i)+0.5*k1);  
    k3 = h*f(t(i)+h/2, w(:,i)+0.5*k2);  
    k4 = h*f(t(i)+h, w(:,i)+k3);  
    w(:,i+1) = w(:,i) + (k1 + 2*k2 + 2*k3 + k4)/6;  
    t(i+1) = a + i*h;  
end
```

```
[t' w']; %transpose matrix
```

```
ts=(1:50);
```

```
tnew=[1 5 10 15 20 25 30 35 40 45 50];
```

```
%experimental results at temperature = 35 degree celcius
```

```
cell=[1.25;2.71;2.89;3.35;3.65;4.14;4.44;4.70;5.27;5.58;7.11;8.33;10.83;11.91;12.57;13  
.63;14.89;15.88;16.94;17.77;19.59;20.42;21.05;21.59;22.93;24.39;25.66;26.90;26.75;2  
7.98;28.05;28.14;29.14;30.14;30.45;30.86;30.98;31.20;31.74;31.86;32.51;32.77;33.19;  
33.41;33.24;33.11;33.00;32.95;32.50;32.50];
```

```
cellnew=[1.25;3.65;5.58;12.57;17.77;22.93;27.98;30.45;31.86;33.24;32.50];
```

```
ethanol=[1.011;1.121;2.021;2.041;2.051;3.061;3.071;3.073;4.079;4.081;4.13;5.74;5.88;  
7.08;8.79;9.97;10.09;12.08;14.40;16.00;17.35;18.42;21.08;20.21;20.83;21.37;21.80;22.  
29;22.67;22.96;23.25;23.59;23.83;24.03;24.27;24.59;24.70;24.95;24.95;25.04;25.24;25  
.33;25.43;25.52;25.62;25.82;25.87;25.92;26.01;26.06];
```

```
ethanolnew=[1.011;2.051;4.081;8.79;16.00;20.83;22.96;24.27;25.04;25.62;26.06];
```

```
sugar=[86.63;86.26;85.82;85.45;85.19;84.74;84.29;83.84;82.93;82.12;81.31;79.78;78.4  
1;76.18;74.37;72.30;70.50;68.43;64.63;62.29;60.59;58.97;57.79;56.80;55.31;54.64;54.  
32;53.74;53.47;53.02;52.84;52.66;52.48;52.48;52.39;52.03;52.03;51.92;51.94;51.89;51  
.66;51.67;51.48;51.39;51.30;51.22;51.31;51.04;50.79;50.01];
```

```
sugarnew=[86.63;85.19;82.12;74.37;62.29;55.31;53.02;52.39;51.89;51.30;50.01];
```

```
plot(t, w(1,:), 'g', t, w(2,:), 'r', t, w(3,:), 'b')
```

```
hold on
```

```
plot(tnew, cellnew, 'o', tnew, ethanolnew, '^', tnew,
```

```
sugarnew, 'square', 'MarkerFaceColor', [1 .5 .1])
```

```
legend('predicted cell', 'predicted ethanol', 'predicted sugar', 'data cell', 'data ethanol', 'data  
sugar')
```

```
%Relative root mean squared error (rRMSE) for model accuracy
```

```
N=50;
```

```
meanCell = sum(cell)/N;
```

```
meanEthanol = sum(ethanol)/N;
```

```
meanSugar = sum(sugar)/N;
```

```
w1=w(1,1:50)';
```

```
w2=w(2,1:50)';
```

```
w3=w(3,1:50)';
```

```
rmseCell=100*(1/meanCell)*sqrt(1/N*sum((w1-cell).^2))
```

```
rmseEthanol=100*(1/meanEthanol)*sqrt(1/N*sum((w2-ethanol).^2))
```

```
rmseSugar=100*(1/meanSugar)*sqrt(1/N*sum((w3-sugar).^2))
```

```
function dy = f(t, y)
```

```
%estimated values
```

```
mum=0.5787;
```

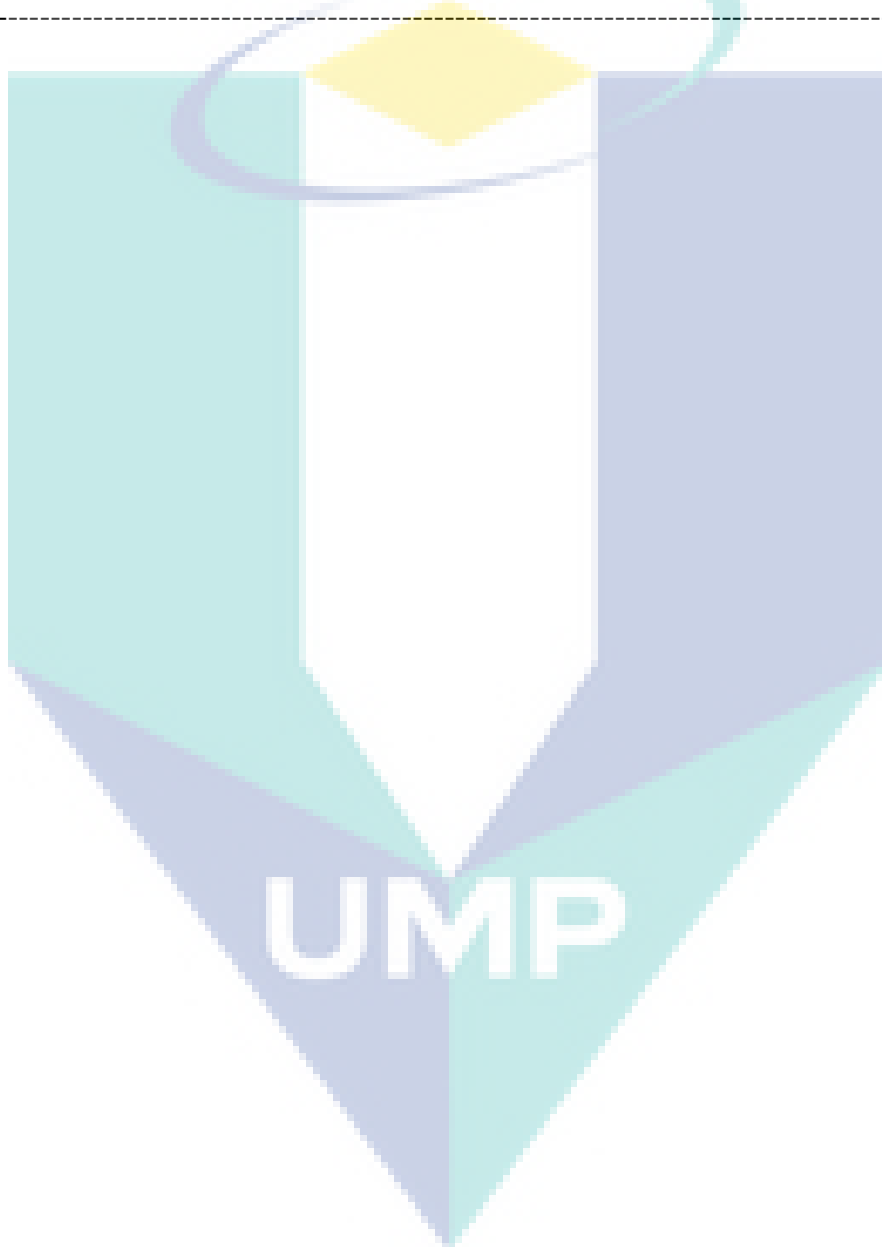
```
ks=0.0956;
```

```
ki=49.6145;
```

```
kd=-0.0072;
```

yps=0.5986;
alpha=0.8459;
pmax=26.06;
n=1.893;

dy =[(mum*y(3)/(ks+y(3)+(y(3)^2/ki))*(1-(y(2)/pmax))^n)*y(1)-kd*y(1);
(alpha*mum*y(3)/(ks+y(3)+(y(3)^2/ki))*(1-(y(2)/pmax))^n)*y(1);
-(alpha*mum*y(3)/((ks+y(3)+(y(3)^2/ki))*yps)*(1-(y(2)/pmax))^n)*y(1)];



APPENDIX B

Model II coding at 25°C temperature

Parameter estimation

```
function S = Sfun2D1(b)
% computation of an error function for an ODE model
% INPUT: b - vector of parameters

global tdata xdata x0

%% ODE model
% (nested function, uses parameters b(1) to b(6) of the main function)
function dx = f(t,x)
    dx = zeros(3,1);
    pmax=29.9024;
    n=3;

    dx(1) = b(1)*x(3)*x(1)/(b(2)+x(3)+(x(3)^2/b(3)))*(1-(x(2)/pmax))^n-b(4)*x(1);
    dx(2)= b(5)*(b(1)*x(3)*x(1)/(b(2)+x(3)+(x(3)^2/b(3)))*(1-(x(2)/pmax))^n-
b(4)*x(1))+b(6)*x(1);
    dx(3)=-((1/b(7))*(b(1)*x(3)*x(1)/(b(2)+x(3)+(x(3)^2/b(3)))*(1-(x(2)/pmax))^n-
b(4)*x(1))+b(8)*x(1));

end

%% numerical integration set up

tspan = [0:1:max(tdata)];
[tsol,xsol] = ode15s(@f,tspan,x0);

%% plot result of the integration

figure(1)
for i = 1:3
    subplot(1,3,i)
    plot(tdata,xdata(:,i),'x','MarkerSize',10);
    hold on
    plot(tsol,xsol(:,i));
    hold off
    ylabel(['x(' num2str(i) ')']);
end

%% find predicted values x(tdata)
```

```
xpred = interp1(tsol,xsol,tdata);
```

```
%% compute total error
```

```
S = 0;
```

```
for i = 1:length(tdata)
```

```
    S = S + sum((xpred(i,:)-xdata(i,:)).^2);
```

```
end
```

```
end
```

```
function paramfit2D
```

```
% main program for fitting parameters of an ODE model to data  
% the model and the error function are defined in the file Sfun2D.m
```

```
global tdata xdata x0
```

```
tdata=(1:50);
```

```
xdata=zeros(50,3);
```

```
xdata(:,1)=[1.25;2.20;3.45;4.76;6.07;7.37;8.74;9.01;11.12;12.43;13.74;15.05;16.30;17.  
55;18.45;19.59;20.73;21.81;22.77;23.63;24.48;25.22;25.84;26.35;26.81;27.15;27.43;28  
.60;28.72;29.72;29.72;30.60;31.47;32.32;32.15;32.86;32.64;32.47;32.18;32.90;33.61;3  
3.39;33.50;33.65;33.82;33.76;33.76;33.76;33.76;33.82];;
```

```
xdata(:,2)=[2.74;3.76;4.73;5.75;6.71;7.74;8.82;9.61;10.63;11.66;12.68;13.70;14.67;15.  
64;16.43;17.28;18.31;19.10;19.95;20.75;21.54;22.23;22.68;23.36;23.93;24.44;24.95;25  
.41;25.81;26.09;26.43;26.77;27.11;27.34;27.57;27.8;28.02;28.14;28.36;28.53;28.70;28.  
82;28.93;29.10;29.22;29.39;29.50;29.61;29.73;29.9024];
```

```
xdata(:,3)=[86.63;82.92;82.48;82.11;81.85;81.4;80.95;80.5;80;78.78;77.97;76.44;75.07  
;72.84;71.03;68.96;67.16;66.5;61.29;58.95;57.25;57;54.45;53.46;51.97;51.3;50.98;50.4  
;50.13;50;49.5;49.32;49.14;49.14;48;48.69;48.69;48.58;48.6;48.7;48.32;48.33;48;48.05  
;47.96;47.88;47.97;47.7;47;46.67];
```

```
%% initial conditions
```

```
x0(1) = 1.25;
```

```
x0(2) = 2.74;
```

```
x0(3) = 86.63;
```

```
%% initial guess of parameter values 25 deg temp
```

```
b = [0.49501 1.1506 220.8311 -0.0099 0.5707 0.0101 0.9302 0.0059];
```

```

%% minimization step

[bmin, Smin] = fminsearch(@Sfun2D1,b);

disp('Estimated parameters b(i):');
disp(bmin)
disp('Smallest value of the error S:');
disp(Smin)

end

function model_25(a, b, N, alpha)

alpha=[1.25 2.74 86.63]; %initial value for y1, y2, and y3
b=50;
a=0;
N=50;

m = size(alpha,1);
if m == 1
    alpha = alpha';
end

h = (b-a)/N; %the step size
t(1) = a;
w(:,1) = alpha; %initial conditions

for i = 1:N
    k1 = h*f(t(i), w(:,i));
    k2 = h*f(t(i)+h/2, w(:,i)+0.5*k1);
    k3 = h*f(t(i)+h/2, w(:,i)+0.5*k2);
    k4 = h*f(t(i)+h, w(:,i)+k3);
    w(:,i+1) = w(:,i) + (k1 + 2*k2 + 2*k3 + k4)/6;
    t(i+1) = a + i*h;
end

[t' w']; %transpose matrix

ts=(1:50);

tnew=[1 5 10 15 20 25 30 35 40 45 50];

%experimental results at temperature = 25 degree celcius

```

```

cell=[1.25;2.20;3.45;4.76;6.07;7.37;8.74;9.01;11.12;12.43;13.74;15.05;16.30;17.55;18.
45;19.59;20.73;21.81;22.77;23.63;24.48;25.22;25.84;26.35;26.81;27.15;27.43;28.60;28
.72;29.72;29.72;30.60;31.47;32.32;32.15;32.86;32.64;32.47;32.18;32.90;33.61;33.39;3
3.50;33.65;33.82;33.76;33.76;33.76;33.76;33.82];
cellnew=[1.25;6.07;12.43;18.45;23.63;26.81;29.72;32.15;32.90;33.82;33.82];
ethanol=[2.74;3.76;4.73;5.75;6.71;7.74;8.82;9.61;10.63;11.66;12.68;13.70;14.67;15.64;
16.43;17.28;18.31;19.10;19.95;20.75;21.54;22.23;22.68;23.36;23.93;24.44;24.95;25.41
;25.81;26.09;26.43;26.77;27.11;27.34;27.57;27.8;28.02;28.14;28.36;28.53;28.70;28.82;
28.93;29.10;29.22;29.39;29.50;29.61;29.73;29.9024];
ethanolnew=[2.74;6.71;11.66;16.43;20.75;23.93;26.09;27.57;28.53;29.22;29.90];
sugar=[86.63;82.92;82.48;82.11;81.85;81.4;80.95;80.5;80;78.78;77.97;76.44;75.07;72.
84;71.03;68.96;67.16;66.5;61.29;58.95;57.25;57;54.45;53.46;51.97;51.3;50.98;50.4;50.
13;50;49.5;49.32;49.14;49.14;48;48.69;48.69;48.58;48.6;48.7;48.32;48.33;48;48.05;47.
96;47.88;47.97;47.7;47;46.67];
sugarnew=[86.63;81.85;78.78;71.03;58.95;51.97;50;48;48.7;47.96;46.67];

```

```

plot(t, w(1,:), 'g', t, w(2,:), 'r', t, w(3,:), 'b')
hold on
plot(tnew, cellnew, 'o', tnew, ethanolnew, '^', tnew,
sugarnew, 'square', 'MarkerFaceColor', [1 .5 .1])
legend('predicted cell', 'predicted ethanol', 'predicted sugar', 'data cell', 'data ethanol', 'data
sugar')

```

%Relative root mean squared error (rRMSE) for model accuracy

```

N=50;
meanCell = sum(cell)/N;
meanEthanol = sum(ethanol)/N;
meanSugar = sum(sugar)/N;

```

```

w1=w(1,1:50); % to make the number of element from rk method is just 50
w2=w(2,1:50);
w3=w(3,1:50);

```

```

rmseCell =100*(1/meanCell)*sqrt(1/N*sum((w1-cell).^2))
rmseEthanol=100*(1/meanEthanol)*sqrt(1/N*sum((w2-ethanol).^2))
rmseSugar=100*(1/meanSugar)*sqrt(1/N*sum((w3-sugar).^2))

```

function dy = f(~, y)

% estimated values

```

mum=1.5845;
ks=5.2053;
ki=27.0843;
kd=-0.0079;

```

```

a=0.6184;
b=0.0072;
yxs=0.8918;
c=0.0037;
n=3;
pmax=29.9024;

```

```

dy = [(mum*y(3)*y(1)/(ks+y(3)+(y(3)^2/ki))*(1-(y(2)/pmax))^n-kd*y(1));
(a*(mum*y(3)*y(1)/(ks+y(3)+(y(3)^2/ki))*(1-(y(2)/pmax))^n-kd*y(1))+b*y(1));
-((1/yxs)*(mum*y(3)*y(1)/(ks+y(3)+(y(3)^2/ki))*(1-(y(2)/pmax))^n-
kd*y(1))+c*y(1))];

```

Model II coding at 30°C temperature

Parameter estimation

```

function S = Sfun2D1(b)
% computation of an error function for an ODE model
% INPUT: b - vector of parameters

global tdata xdata x0

%% ODE model
% (nested function, uses parameters b(1) to b(6) of the main function)
function dx = f(t,x)
    dx = zeros(3,1);
    pmax=30.76;
    n=3;

    dx(1) = b(1)*x(3)*x(1)/(b(2)+x(3)+(x(3)^2/b(3)))*(1-(x(2)/pmax))^n-b(4)*x(1);
    dx(2) = b(5)*(b(1)*x(3)*x(1)/(b(2)+x(3)+(x(3)^2/b(3)))*(1-(x(2)/pmax))^n-
    b(4)*x(1))+b(6)*x(1);
    dx(3) = -((1/b(7))*(b(1)*x(3)*x(1)/(b(2)+x(3)+(x(3)^2/b(3)))*(1-(x(2)/pmax))^n-
    b(4)*x(1))+b(8)*x(1));

end

%% numerical integration set up

tspan = [0:1:max(tdata)];
[tsol,xsol] = ode15s(@f,tspan,x0);

```



```

%% plot result of the integration

figure(1)
for i = 1:3
    subplot(1,3,i)
    plot(tdata,xdata(:,i),'x','MarkerSize',10);
    hold on
    plot(tsol,xsol(:,i));
    hold off
    ylabel(['x(' num2str(i) ')']);
end

%% find predicted values x(tdata)
xpred = interp1(tsol,xsol,tdata);

%% compute total error
S = 0;
for i = 1:length(tdata)
    S = S + sum((xpred(i,:)-xdata(i,:)).^2);
end

end

-----

function paramfit2D

% main program for fitting parameters of an ODE model to data
% the model and the error function are defined in the file Sfun2D.m

global tdata xdata x0

tdata=(1:50);
xdata=zeros(50,3);
xdata
(:,1)=[1.25;5.66;7.16;8.54;10.14;11.81;13.41;15.08;16.47;18.13;19.74;21.36;22.67;24.2
8;25.74;27.15;28.36;29.63;30.89;32.69;33.02;34;35.32;35.56;36.18;36.76;37.15;37.67;
37.73;37.9;38.02;38.13;38.13;38.02;37.95;37.79;37.6;37.5;37.33;37.04;36.87;36.64;36.
64;36.24;36.06;35.95;35.76;35.8;35.66;35.6];
xdata
(:,2)=[4.30;5.28;6.31;7.12;8.15;9.24;10.28;11.31;12.23;13.21;14.24;15.11;16.20;17.23;
18.15;19.07;19.88;20.68;21.54;22.29;22.92;23.61;24.19;24.73;25.16;25.62;26.03;26.37
;26.54;26.83;27.06;27.23;27.35;27.46;27.52;27.63;27.63;27.63;27.69;28.69;28.69;28.8
1;29.38;29.84;30.19;30.76;29.30;29.01;28.61;28.38];
xdata
(:,3)=[86.63;82.03;79.50;77.96;77.51;77.06;75.03;73.85;72.08;71.50;70.18;69.03;68.20

```

```
;67.35;66.05;64.45;63.31;60.04;57.40;55.06;53.36;53.11;50.56;49.57;48.08;47.41;47.0  
9;46.51;46.24;46.11;45.61;45.43;45.25;45.25;44.11;44.80;44.80;44.69;44.71;44.81;44.  
43;44.44;44.11;44.16;44.07;43.99;44.08;43.81;43.11;42.78];
```

```
%% initial conditions
```

```
x0(1) = 1.25;  
x0(2) = 4.30;  
x0(3) = 86.63;
```

```
%% initial guess of parameter values 30 deg temp
```

```
b = [0.6901 2.1006 229.8311 -0.0091 0.5007 0.0101 0.9002 0.0049];
```

```
%% minimization step
```

```
[bmin, Smin] = fminsearch(@Sfun2D1,b);
```

```
disp('Estimated parameters b(i):');  
disp(bmin)  
disp('Smallest value of the error S:');  
disp(Smin)
```

```
end
```

Main coding

```
function model_30(a, b, N, alpha)
```

```
alpha=[1.25 4.30 86.63]; %initial value for y1, y2, and y3  
b=50;  
a=0;  
N=50;
```

```
m = size(alpha,1);  
if m == 1  
    alpha = alpha';  
end
```

```
h = (b-a)/N; %the step size  
t(1) = a;  
w(:,1) = alpha; %initial conditions
```

```
for i = 1:N
```

```

k1 = h*f(t(i), w(:,i));
k2 = h*f(t(i)+h/2, w(:,i)+0.5*k1);
k3 = h*f(t(i)+h/2, w(:,i)+0.5*k2);
k4 = h*f(t(i)+h, w(:,i)+k3);
w(:,i+1) = w(:,i) + (k1 + 2*k2 + 2*k3 + k4)/6;
t(i+1) = a + i*h;
end

%w(1,:), w(2,:), w(3,:) listing for y(1), y(2), and y(3) respectively

[t' w']; %transpose matrix
ts=(1:50);
tnew=[1 5 10 15 20 25 30 35 40 45 50];

%experimental results at temperature = 30 degree celcius

cell=[1.25;5.66;7.16;8.54;10.14;11.81;13.41;15.08;16.47;18.13;19.74;21.36;22.67;24.2
8;25.74;27.15;28.36;29.63;30.89;32.69;33.02;34;35.32;35.56;36.18;36.76;37.15;37.67;
37.73;37.9;38.02;38.13;38.13;38.02;37.95;37.79;37.6;37.5;37.33;37.04;36.87;36.64;36.
64;36.24;36.06;35.95;35.76;35.8;35.66;35.6];
cellnew=[1.25;10.14;18.13;25.74;32.69;36.18;37.9;37.95;37.04;36.06;35.6];
ethanol=[4.30;5.28;6.31;7.12;8.15;9.24;10.28;11.31;12.23;13.21;14.24;15.11;16.20;17.
23;18.15;19.07;19.88;20.68;21.54;22.29;22.92;23.61;24.19;24.73;25.16;25.62;26.03;26
.37;26.54;26.83;27.06;27.23;27.35;27.46;27.52;27.63;27.63;27.63;27.69;28.69;28.69;2
8.81;29.38;29.84;30.19;30.76;29.30;29.01;28.61;28.38];
ethanolnew=[4.30;8.15;13.21;18.15;22.29;25.16;26.83;27.52;28.69;30.19;28.38];
sugar=[86.63;82.03;79.50;77.96;77.51;77.06;75.03;73.85;72.08;71.50;70.18;69.03;68.2
0;67.35;66.05;64.45;63.31;60.04;57.40;55.06;53.36;53.11;50.56;49.57;48.08;47.41;47.
09;46.51;46.24;46.11;45.61;45.43;45.25;45.25;44.11;44.80;44.80;44.69;44.71;44.81;44
.43;44.44;44.11;44.16;44.07;43.99;44.08;43.81;43.11;42.78];
sugarnew=[86.63;77.51;71.50;66.05;55.06;48.08;46.11;44.11;44.81;44.07;42.78];

plot(t, w(1,:), 'g', t, w(2,:), 'r', t, w(3,:), 'b')
hold on
plot(tnew, cellnew, 'o', tnew, ethanolnew, '^', tnew,
sugarnew, 'square', 'MarkerFaceColor', [.1 .5 .1])
legend('predicted cell', 'predicted ethanol', 'predicted sugar', 'data cell', 'data ethanol', 'data
sugar')

%Relative root mean squared error (rRMSE) for model accuracy

N=50;
meanCell = sum(cell)/N;
meanEthanol = sum(ethanol)/N;
meanSugar = sum(sugar)/N;

```

```
w1=w(1,1:50)'; % to make the number of element from rk method is just 50
w2=w(2,1:50)';
w3=w(3,1:50)';
```

```
rmseCell=100*(1/meanCell)*sqrt(1/N*sum((w1-cell).^2))
rmseEthanol=100*(1/meanEthanol)*sqrt(1/N*sum((w2-ethanol).^2))
rmseSugar=100*(1/meanSugar)*sqrt(1/N*sum((w3-sugar).^2))
```

```
function dy = f(t, y)
```

```
%estimated values
```

```
mum=0.7821;
ks=1.3832;
ki=290.4042;
kd=0.0005;
a=0.4414;
b=0.0075;
yxs=1.1250 ;
c=0.0097;
n=3;
pmax=30.76;
```

```
dy = [(mum*y(3)*y(1)/(ks+y(3)+(y(3)^2/ki))*(1-(y(2)/pmax))^n-kd*y(1));
(a*(mum*y(3)*y(1)/(ks+y(3)+(y(3)^2/ki))*(1-(y(2)/pmax))^n-kd*y(1))+b*y(1));
-((1/yxs)*(mum*y(3)*y(1)/(ks+y(3)+(y(3)^2/ki))*(1-(y(2)/pmax))^n-
kd*y(1))+c*y(1))];
```

Model II coding at 35°C temperature

Parameter estimation

```
function S = Sfun2D1(b)
% computation of an error function for an ODE model
% INPUT: b - vector of parameters

global tdata xdata x0

%% ODE model
% (nested function, uses parameters b(1) and b(2) of the main function)
function dx = f(t,x)
    dx = zeros(3,1);
    pmax=26.06;
    n=3;

    dx(1) = b(1)*x(3)*x(1)/(b(2)+x(3)+(x(3)^2/b(3)))*(1-(x(2)/pmax))^n-b(4)*x(1);
    dx(2) = b(5)*(b(1)*x(3)*x(1)/(b(2)+x(3)+(x(3)^2/b(3)))*(1-(x(2)/pmax))^n-
b(4)*x(1))+b(6)*x(1);
    dx(3) = -(1/b(7))*(b(1)*x(3)*x(1)/(b(2)+x(3)+(x(3)^2/b(3)))*(1-(x(2)/pmax))^n-
b(4)*x(1))+b(8)*x(1);

end

%% numerical integration set up

tspan = [0:1:max(tdata)];
[tsol,xsol] = ode15s(@f,tspan,x0);

%% plot result of the integration
figure(1)
for i = 1:3
    subplot(1,3,i)
    plot(tdata,xdata(:,i),'x','MarkerSize',10);
    hold on
    plot(tsol,xsol(:,i));
    hold off
    ylabel(['x(' num2str(i) ')']);
end

%% find predicted values x(tdata)

xpred = interp1(tsol,xsol,tdata);

%% compute total error

S = 0;
for i = 1:length(tdata)
    S = S + sum((xpred(i,:)-xdata(i,:)).^2);
end
```

end

end

```
function paramfit2D
```

```
% main program for fitting parameters of an ODE model to data  
% the model and the error function are defined in the file Sfun2D.m
```

```
%clearvars -global  
global tdata xdata x0
```

```
tdata=(1:50);  
xdata=zeros(50,3);  
xdata(:,1)=[1.25;2.71;2.89;3.35;3.65;4.14;4.44;4.70;5.27;5.58;7.11;8.33;10.83;11.91;12  
.57;13.63;14.89;15.88;16.94;17.77;19.59;20.42;21.05;21.59;22.93;24.39;25.66;26.90;2  
6.75;27.98;28.05;28.14;29.14;30.14;30.45;30.86;30.98;31.20;31.74;31.86;32.51;32.77;  
33.19;33.41;33.24;33.11;33.00;32.95;32.50;32.50];  
xdata  
(:,2)=[1.011;1.121;2.021;2.041;2.051;3.061;3.071;3.073;4.079;4.081;4.13;5.74;5.88;7.0  
8;8.79;9.97;10.09;12.08;14.40;16.00;17.35;18.42;21.08;20.21;20.83;21.37;21.80;22.29;  
22.67;22.96;23.25;23.59;23.83;24.03;24.27;24.59;24.70;24.95;24.95;25.04;25.24;25.33  
;25.43;25.52;25.62;25.82;25.87;25.92;26.01;26.06];  
xdata  
(:,3)=[86.63;86.26;85.82;85.45;85.19;84.74;84.29;83.84;82.93;82.12;81.31;79.78;78.41  
;76.18;74.37;72.30;70.50;68.43;64.63;62.29;60.59;58.97;57.79;56.80;55.31;54.64;54.3  
2;53.74;53.47;53.02;52.84;52.66;52.48;52.48;52.39;52.03;52.03;51.92;51.94;51.89;51.  
66;51.67;51.48;51.39;51.30;51.22;51.31;51.04;50.79;50.01];
```

```
%% initial conditions
```

```
x0(1) = 1.25;  
x0(2) = 1.011;  
x0(3) = 86.63;
```

```
%% initial guess of parameter values 35 deg temp
```

```
b = [0.4001 3.2506 235.8311 -0.0110 0.5607 0.0101 0.9502 0.0045];
```

```
%% minimization step
```

```
[bmin, Smin] = fminsearch(@Sfun2D1,b);
```

```
disp('Estimated parameters b(i):');
```

```

disp(bmin)
disp('Smallest value of the error S:');
disp(Smin)

```

```
end
```

Main coding

```

function model_35(a, b, N, alpha)

alpha=[1.25 1.011 86.63]; %initial value for y1, y2, and y3
b=50;
a=0;
N=50;

m = size(alpha,1);
if m == 1
    alpha = alpha';
end

h = (b-a)/N; %the step size
t(1) = a;
w(:,1) = alpha; %initial conditions

for i = 1:N
    k1 = h*f(t(i), w(:,i));
    k2 = h*f(t(i)+h/2, w(:,i)+0.5*k1);
    k3 = h*f(t(i)+h/2, w(:,i)+0.5*k2);
    k4 = h*f(t(i)+h, w(:,i)+k3);
    w(:,i+1) = w(:,i) + (k1 + 2*k2 + 2*k3 + k4)/6;
    t(i+1) = a + i*h;
end

%w(1,:), w(2,:), w(3,:) listing for y(1), y(2), and y(3) respectively

[t' w']; %transpose matrix

ts=(1:50);

tnew=[1 5 10 15 20 25 30 35 40 45 50];

%experimental results at temperature = 35 degree celcius

cell=[1.25;2.71;2.89;3.35;3.65;4.14;4.44;4.70;5.27;5.58;7.11;8.33;10.83;11.91;12.57;13
.63;14.89;15.88;16.94;17.77;19.59;20.42;21.05;21.59;22.93;24.39;25.66;26.90;26.75;2
7.98;28.05;28.14;29.14;30.14;30.45;30.86;30.98;31.20;31.74;31.86;32.51;32.77;33.19;
33.41;33.24;33.11;33.00;32.95;32.50;32.50];

```

```

cellnew=[1.25;3.65;5.58;12.57;17.77;22.93;27.98;30.45;31.86;33.24;32.50];
ethanol=[1.011;1.121;2.021;2.041;2.051;3.061;3.071;3.073;4.079;4.081;4.13;5.74;5.88;
7.08;8.79;9.97;10.09;12.08;14.40;16.00;17.35;18.42;21.08;20.21;20.83;21.37;21.80;22.
29;22.67;22.96;23.25;23.59;23.83;24.03;24.27;24.59;24.70;24.95;24.95;25.04;25.24;25
.33;25.43;25.52;25.62;25.82;25.87;25.92;26.01;26.06];
ethanolnew=[1.011;2.051;4.081;8.79;16.00;20.83;22.96;24.27;25.04;25.62;26.06];
sugar=[86.63;86.26;85.82;85.45;85.19;84.74;84.29;83.84;82.93;82.12;81.31;79.78;78.4
1;76.18;74.37;72.30;70.50;68.43;64.63;62.29;60.59;58.97;57.79;56.80;55.31;54.64;54.
32;53.74;53.47;53.02;52.84;52.66;52.48;52.48;52.39;52.03;52.03;51.92;51.94;51.89;51
.66;51.67;51.48;51.39;51.30;51.22;51.31;51.04;50.79;50.01];
sugarnew=[86.63;85.19;82.12;74.37;62.29;55.31;53.02;52.39;51.89;51.30;50.01];

```

```

plot(t, w(1,:), 'g', t, w(2,:), 'r', t, w(3,:), 'b')
hold on
plot(tnew, cellnew, 'o', tnew, ethanolnew, '^', tnew,
sugarnew, 'square', 'MarkerFaceColor', [1 .5 .1])
legend('predicted cell', 'predicted ethanol', 'predicted sugar', 'data cell', 'data ethanol', 'data
sugar')
%Relative root mean squared error (rRMSE) for model accuracy

```

```

N=50;
meanCell = sum(cell)/N;
meanEthanol = sum(ethanol)/N;
meanSugar = sum(sugar)/N;

```

```

w1=w(1,1:50); % to make the number of element from rk method is just 50
w2=w(2,1:50);
w3=w(3,1:50);

```

```

rrmseCell=100*(1/meanCell)*sqrt(1/N*sum((w1-cell).^2))
rrmseEthanol=100*(1/meanEthanol)*sqrt(1/N*sum((w2-ethanol).^2))
rrmseSugar=100*(1/meanSugar)*sqrt(1/N*sum((w3-sugar).^2))

```

```

function dy = f(t, y)

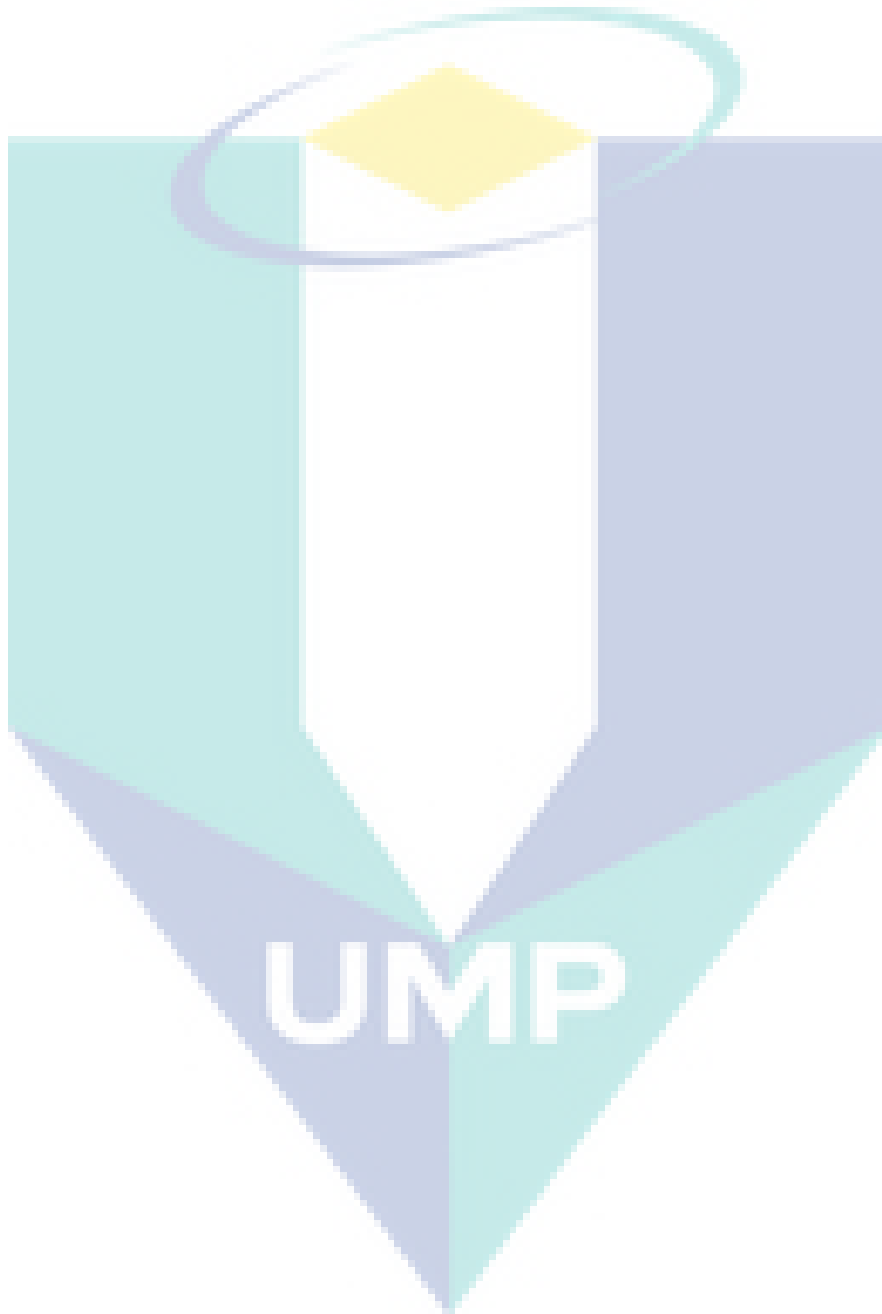
```

```

%estimated values
mum=0.5065;
ks=8.7677;
ki=71.2317;
kd=-0.0117;
a=0.4475;
b=0.0140;
yxs=0.7308 ;
c=-0.0087;
n=3;
pmax=26.06;

```


$$\begin{aligned}
 dy = & [(mum*y(3)*y(1)/(ks+y(3)+(y(3)^2/ki))*(1-(y(2)/pmax))^n-kd*y(1)); \\
 & (a*(mum*y(3)*y(1)/(ks+y(3)+(y(3)^2/ki))*(1-(y(2)/pmax))^n-kd*y(1)+b*y(1)); \\
 & -((1/yxs)*(mum*y(3)*y(1)/(ks+y(3)+(y(3)^2/ki))*(1-(y(2)/pmax))^n- \\
 & kd*y(1))+c*y(1)];
 \end{aligned}$$



APPENDIX C

Publication

S Sultana, Norazaliza Mohd Jamil, E A M Saleh, A Yousuf, Che Ku M Faizal, A mathematical model for ethanol fermentation from oil palm trunk sap using *Saccharomyces cerevisiae*, *Journal of Physics: Conference Series*, 890, 012050, 2017. (Scopus Indexed)

